Published in final edited form as:
Front Biosci. ; 13: 4558–4575.

ADVANCES IN MOLECULAR IMAGING OF PANCREATIC BETA CELLS

Mai Lin[1], **Angelo Lubag**[2], **Michael J. McGuire**[3], **Serguei Y. Seliounine**[1], **Edward N. Tsyganov**[1], **Peter P. Antich**[1], **A. Dean Sherry**[2,4], **Kathlynn C. Brown**[3,*], and **Xiankai Sun**[1,*]

[1]Department of Radiology, University of Texas Southwestern Medical Center, 5323 Harry Hines Blvd., Dallas, Texas 75390, USA

[2]The Advanced Imaging Research Center, University of Texas Southwestern Medical Center, 5323 Harry Hines Blvd., Dallas, Texas 75390, USA

[3]Department of Internal Medicine, University of Texas Southwestern Medical Center, 5323 Harry Hines Blvd., Dallas, Texas 75390, USA

[4]Department of Chemistry, University of Teas at Dallas, Richardson, Texas 75083, USA

Abstract

The development of non-invasive imaging methods for early diagnosis of the beta cell associated metabolic diseases, including type 1 and type 2 diabetes (T1D and T2D), has recently drawn considerable interest from the molecular imaging community as well as clinical investigators. Due to the challenges imposed by the location of the pancreas, the sparsely dispersed beta cell population within the pancreas, and the poor understanding of the pathogenesis of the diseases, clinical diagnosis of beta cell abnormalities is still limited. Current diagnostic methods are invasive, often inaccurate, and usually performed post-onset of the disease. Advances in imaging techniques for probing beta cell mass and function are needed to address this critical health care problem. A variety of currently available imaging techniques have been tested for the assessment of the pancreatic beta cell islets. Here we discuss the current advances in magnetic resonance imaging (MRI), bioluminescence imaging (BLI), and nuclear imaging for the study of beta cell diseases. Spurred by early successes in nuclear imaging techniques for beta cells, especially positron emission tomography (PET), the need for beta cell specific ligands has expanded. Progress in the field for obtaining such ligands is presented. Additionally, we report our preliminary efforts of developing such a peptidic ligand for PET imaging of the pancreatic beta cells.

2. INTRODUCTION

According to the statistics published by the American Diabetes Association (ADA), diabetes is the fifth leading cause of death by disease in the United States, contributing to a total 224,092 deaths in the United States alone in 2002 (1). People with diabetes are at significantly higher risk to develop heart disease and stroke, high blood pressure, blindness, kidney failure, nervous system disease, and other chronic complications that severely affect the life quality of the patients. Being a chronic disease without a cure, diabetes now affects 7.0% of the population in the United States, or 20.8 million children and adults, among which 6.2 million people were

Send correspondence to: Kathlynn C. Brown, Department of Internal Medicine, University of Texas Southwestern Medical Center, 5323 Harry Hines Blvd., Dallas, Texas 75390-9185, USA; Tel: (+)1-214-648-1807; Fax: (+)1-214-648-4156; Kathlynn.Brown@UTSouthwestern.edu, Xiankai Sun, Department of Radiology, University of Texas Southwestern Medical Center, 5323 Harry Hines Blvd., Dallas, Texas 75390-9058, USA; Tel: (+)1-214-648-2909; Fax: (+)1-214-648-4538; Xiankai.Sun@UTSouthwestern.edu.

undiagnosed. The national medical cost attributable to diabetes was estimated at $132 billion by the ADA in 2002. Both the prevalence of diabetes and the annual expenditures of diabetes-associated care are projected to climb in foreseeable future (1).

Diabetes is hallmarked by high levels of blood glucose caused by lack of insulin production, insulin resistance in peripheral tissues, or both. The insulin producing beta cells that govern glucose homeostasis are located in the islets of Langerhans which make up only 2 – 3 % of all pancreatic tissues. Beta cells represent ~ 80% of the islets, while other types of cells (mainly alpha, delta, and PP cells) contribute to the remaining 20%. In humans, the pancreas is a small elongated pinkish organ in the abdomen neighboring the liver, duodenum, stomach, and spleen.

There are two major forms of diabetes. Type 1 diabetes (T1D), also known as juvenile diabetes, is usually found in children and young adults. It results from a T-cell mediated autoimmune attack on the beta cells (2,3). Type 2 diabetes (T2D) is the most common form of diabetes accounting for 90 – 95% of all diagnosed cases. T2D begins with insulin resistance in peripheral tissues, a gradual increase in circulating blood glucose that triggers beta cells to release even more insulin, and subsequent failure of beta cells to maintain normal glucose homeostasis (4). While the onset of T1D is directly reflected by the loss of the pancreatic beta cells, T2D consists of multiple metabolic abnormalities leading to hyperglycemia.

It has been shown islet cell autoantibodies are strongly associated with the development of T1D and insulinitis concurs with an inflammatory infiltration of mononuclear cells (5,6). The appearance of autoantibodies to one or several autoantigens signals the autoimmune pathogenesis of beta cell destruction. Although genetic susceptibility appears to be a prerequisite of developing T1D, studies of identical twins have shown that the concordance rate of the disease is only 40% (7), suggesting that other environmental factors are involved in the initiation and/or progression of T1D. To date, 14 different viruses have been reported to be involved in the development of T1D in humans and animal models (8). Viruses may either trigger beta cell specific autoimmunity leading to diabetes or directly infect and destroy beta cells resulting in T1D.

Several cellular or molecular mechanisms have been reported to be associated with T2D, such as reduced expression of insulin receptors on the surface of insulin-responsive cells (9–12), alterations in the signal-transduction pathways of insulin action (13–16), and abnormalities in biologic pathways normally stimulated by insulin (17–20). In addition, mutations in the insulin-receptor gene are responsible for insulin resistance in some people (21).

In spite of the tremendous progress in understanding the basis of diabetes, there is still no known cure. It remains unclear what factors are involved in the disease development and govern the response to therapeutic intervention. With the recent technical innovations in various imaging modalities, molecular imaging is gaining more attention in the basic biomedical sciences and in clinical research and practice (21–24). Indeed, non-invasive imaging techniques are revolutionizing the understanding of diseases at the cellular and molecular levels. The ability to non-invasively visualize beta cells would greatly facilitate the development of new methods in the prevention and treatment of diabetes (22,23).

3. TECHNIQUES FOR IMAGING THE PANCREATIC BETA CELLS

There is considerable interest in using recently developed imaging techniques to monitor the pancreatic beta cells mass and function non-invasively (22–49). Conventional magnetic resonance imaging (MRI) and computed tomography can be used to delineate the location of the pancreas in a subject at a spatial resolution of less than 100 micrometers. However, it is extremely difficult, if not impossible, for these two modalities to differentiate the islets of Langerhans from other pancreatic tissues because the pancreas is a highly vascularized soft

organ and the islets of Langerhans only represent 2 – 3 % of the pancreas tissues. In order to visualize beta cells in the islets of Langerhans, imaging or contrast agents that recognize the scarcely dispensed beta cells within the pancreas and/or are responsive to their biological functions must be developed.

3.1. Magnetic Resonance Imaging Methods

New methods have been developed in recent years to overcome the sensitivity limit of MRI for the assessment of the pancreatic beta cells. In 2002, Moore and coworkers first reported a sensitivity-enhancing method to distinguish the endocrine from exocrine tissues and monitor cell infiltration in the pancreatic islets (25). This approach employs mouse lymphocytes labeled with cross-linked iron oxide nanoparticles (CLIO) to enhance the T_2 contrast of MR images. After adoptive transfer of the labeled cells to NOD/SCID mice, pancreatic tissues were excised and the MR images were obtained *ex vivo*. The investigators further applied this approach to visualize insulinitic lesions that consist predominantly of cytotoxic $CD8^+$ T cells (33). As shown in Figure 1, the MRI contrast agent was constructed by attaching multiple copies of a synthetic peptide (NRP) that targets beta cell autoantigens to the surface of CLIO via the interaction between biotin and avidin. The images acquired in live NOD diabetic-prone mice showed that the $CD8^+$ T cells were tracked in the pancreatic tissues (33).

Superparamagnetic iron oxide nanoparticles (SPIO) have also been used to label islet transplants and longitudinally monitor their fate non-invasively. Saudek and coworkers labeled beta cell islets with commercial SPIO and transplanted them into livers of experimental rats via the portal vein (30,39). The SPIO-labeled islets were clearly visible in the liver of both healthy and diabetic rats up to 22 weeks by MRI. It was also observed that the blood glucose levels in diabetic rats were significantly decreased after islet transplantation, indicating that the SPIO particles did not destroy the functionality of beta cell islets. They further used this method to longitudinally monitor *in vivo* tolerance of transplanted pancreatic islets in both syngeneic and allogeneic rat models (40). Within seven days post transplantation, the allogeneic animals exhibited similar MRI islet patterns to the animals in the syngeneic group; all animals remained normoglycemic. By day 12, all the allogeneic animals turned diabetic and the detectable transplanted islet spots on MR images became significantly fewer at 14 days post transplantation. In contrast, the syngeneic animals remained norglycemic and the number of transplanted islets detected by MRI remained relatively constant over the entire six week study period (40). This clearly shows that MRI methods using SPIO labeled islets can be used to non-invasively detect *in vivo* tolerance and rejection of islet transplants.

Insulin secretion from the pancreatic beta cell is a Ca^{2+}-dependent event. Recently, Roman and coworkers reported an enhanced MR method using Mn^{2+} as a paramagnetic surrogate of Ca^{2+} to assess beta cell function in a cell culture as well as in isolated mouse islets (44). Exogeneous Mn^{2+} appears to be taken into beta cells *via* Ca^{2+} channels and this results in a 200% increase in contrast in T_1 weighted MR images upon stimulating the cells or islets with D-glucose for insulin secretion (44).

In 2000, Balaban and coworkers reported a method to alter image contrast via chemical exchange saturation transfer (CEST) of pre-saturated slowly exchanging –NH or OH proton spins of MRI contrast agents to bulk water (50,51). Due to the small chemical shift difference (typically < 5 ppm) between the exchanging –NH and –OH protons in diamagnetic molecules and bulk water, it is difficult to apply CEST in tissues where the bulk water resonance has broadened baseline (38). However, Sherry and others have demonstrated that in some paramagnetic lanthanide complexes, the bound water resonance is shifted as much as 800 ppm away from the bulk water resonance (38,52–66). Importantly the MR image contrast of such paramagnetic CEST agents (PARACEST) is largely determined by the chemical exchange characteristics of lanthanide complexes and to much less extent their relaxation properties

(60). This has opened a novel avenue to design biologically responsive MR imaging agents. Indeed, a PARACEST agent, EuDTMA-2PB^{3+} (Figure 2), is able to map tissue glucose by CEST imaging (61). Physiological concentrations of glucose can be potentially quantified by using a clinical MR scanner and this europium complex.

3.2. Optical Imaging Methods

Current optical imaging techniques include the well developed systems of confocal microscopy and optical coherent tomography for the studies of superficial tissues and cells, and reflectance imaging and diffuse optical tomography to image deep tissues (27). Recently a number of research groups have successfully applied these methods to study the biology and function of beta cells in the intact pancreas (27,67–70) and in transplanted islets (23,27,36,43,46,71–74). There are two chief ways of enabling optical imaging studies: (1) transfect the islets with reporter genes that produce light-emitting proteins upon external light excitation (e.g. green fluorescence protein) or enzymes that act on substrates (e.g. luciferase and luciferin) to emit visible light; (2) develop targeted molecular beacons that absorb external light of one wavelength and emit light at another wavelength with high efficiency.

To date, *in vivo* bioluminescence imaging (BLI) has been utilized by various groups for the assessment of pancreatic beta cell mass after islet transplantation (29,36,46,71,73). To image and quantify transplanted islets by BLI, healthy murine or human islets are transfected by adenovirus-mediated gene transfer to express luciferase prior to transplantation. As reported by Powers and coworkers, the survival of transplanted human or murine islets in NOD-SCID mice could be quantitatively assessed by BLI up to eighteen weeks (73). However, it was also reported that luciferase expression after adenovirus-mediated gene transfer is transient and attenuates ~10-fold starting from 2 days post transplantation while luminescence is relatively stable out to ten days post transplantation (75). Lentivirus has also been tested for the gene transfer. While lentivirus provided longer lasting luciferase expression than infection by adenovirus, the viral transduction efficiency of lentivirus was lower (75). It is noteworthy that Park and coworkers recently established a transgenic mouse model (MIP-*luc*) by introducing the mouse insulin I promoter (MIP)-luciferase transgenic construct into the pronucli of fertilized oocytes from CD-1 mice (76). The transgenic mice have normal glucose tolerance and pancreatic architecture. Importantly, luciferase expression was only observed in the pancreatic islets not in other organs. It is expected that such a transgenic animal model would be useful for the real time studies of beta cell function under different physiological conditions using *in vivo* BLI (76).

The available chromophores that could be used to develop molecular beacons for optical imaging have been thoroughly reviewed by Achilefu (27). Considering that the pancreas is deep within the abdomen, the chromophores that emit near infrared radiation (NIR: 700 – 900 nm) are preferred for reasons of tissue penetration. By conjugating a commercially available NIR dye, Cy5.5, with annexin V, Moore and coworkers were able to detect the difference levels of apoptosis of beta cell islets between diabetic and control animals in the animal models of both TID and T2D *in vitro* and *ex vivo*. Because annexin V is an early marker of apoptosis, such a NIR probe may enable the early detection of diabetic beta cell death (77). The same group also reported a dual modality method to non-invasively monitor transplanted human pancreatic islets under the kidney capsule of NOD-SCID mice by labeling the islets with Cy5.5 modified SPIO nanoparticles (78). However, *in vivo* detection was performed by MRI, while the optical imaging was used only to confirm the presence of the imaging probe in the graft and to differentiate labeled *versus* nonlabeled islets *ex vivo*.

3.3. Nuclear Imaging Methods

It has been reported that a glycogen pool exists in insulin-producing beta cells but not in acinar cells in spontaneously diabetic animals (79–81). Therefore as early as in 2000, the most commonly used PET imaging probe, ^{18}F-FDG (2-deoxy-2-^{18}F-fluoro-D-glucose) (^{18}F: $t_{1/2}$ = 109 min), was used by Malaisse and coworkers for imaging and quantification of the endocrine pancreas in rats (82,83). Based on the fact that the phosphorylated ^{18}F-FDG cannot proceed further in the glycolytic pathway, an elevated accumulation in the glycogen pool was expected. Following intravenous injection, uptake of ^{18}F-FDG in various organs of interest was examined. It was found that indeed the accumulation of ^{18}F-FDG in the rat pancreas was three times the paired plasma value at 4 h post injection. However this elevated pancreas uptake in rats could not be reproduced in the subsequent human studies (84). Malaisse and others have resorted to other radiolabeled monosaccharides, such as D-mannoheptulose, for the selection of suitable candidates for *in vivo* imaging of the pancreatic beta cells (41,84–95). In rodents, uptake of tritiated D-mannoheptulose in liver and transplanted islets was found up to eight times higher than the paired value found in pancreas (96). Hence, Malaisse and coworkers designed several nuclear imaging probes based on D-mannoheptulose, such as 1-^{11}C-labeled-D-mannoheptulose, 3-deoxy-3-^{18}F-fluoro-D- mannoheptulose, and 7-deoxy-7-^{123}I-iodo-D-mannoheptulose (41,84,87). The radiochemical preparation and *in vivo* evaluation of these PET/SPECT tracers have not been reported to date.

In addition to saccharide derivatives, Malaisse and coworkers also used an ^{125}I labeled monoclonal antibody directed against rat islet beta cell plasma membrane for selective imaging of the pancreatic beta cells by SPECT (97). The radiolabeled antibody showed approximately one order of magnitude higher uptake in isolated islets than in acinar tissue but this difference was found nearly the same in the tissues obtained from control and diabetic rats, indicating that antibody uptake could not reflect a reduction in the number of beta cell islets in the diabetic pancreas. Not surprisingly, no significant difference of pancreas uptake was observed in *in vivo* studies performed from 1 to 4 days post injection.

Sweet and coworkers recently attempted to use another existing beta cell specific antibody (K14D10) for the assessment of pancreatic beta cell mass (98). Considering that antibody fragments usually have better blood clearance that may improve the desired pancreas contrast, they evaluated a fragment of the antibody as well. Although the fragment and the intact antibody showed similar binding affinity to beta cells (6 – 20 nM), their low binding specificity to beta cells *versus* exocrine cells did not warrant further *in vivo* evaluation.

A successful attempt of using monoclonal antibodies for beta cell imaging was reported by Moore and coworker in 2001 (99). They used the beta cell specific antibody, IC2, which had shown exclusive binding to the surface membrane of beta cells (100–102). The antibody was conjugated to a bifunctional chelator, diethylenetriamine pentaacetic acid (DTPA), then labeled with ^{111}In. Both *in vitro* and *in vivo* evaluations showed that accumulation of ^{111}In-DTPA-IC2 was specific to beta cells. More impressively, the imaging probe uptake in the islet beta cells showed a positive correlation (r^2 = 0.936) with the reduction of beta cell mass in the diabetic rats. This correlation was further confirmed by *ex vivo* nuclear imaging of excised organs at 24 h post intravenous injection of the ^{111}In-labeled antibody. In spite of the promising results, the major drawback of this study is the nuclear imaging was not carried out in live animals. As the authors indicate, further work, such as modification of the probe and mechanistic studies of the antibody's specificity, needs to be done for future practical clinical applications.

By analogy to *in vivo* BLI, the method of reporter gene transfer has also been applied to nuclear imaging of beta cell islets, where the reporter gene was herpes simplex virus type 1 thymidine kinase (HSV1-TK), a common suicide gene used for cancer gene therapy (103,104). Nuclear

imaging probes have been reported for non-invasively imaging HSV1-TK gene expression (105–108). Among them, ^{18}F-labeled FHBG (9-(4-^{18}F-fluro-3-hydroxymethylbutyl)guanine) and iodine radioisotope-labeled FIAU (5-^{123,124,131}I-iodo-2'-fluoro-2'-deoxy-1-β-D-arabinofuranosyluracil) are the most commonly used tracers (Figure 3). After intravenous injection, these nuclear imaging probes are monophosphorylated by thymidine kinase expressed in tissues transfected by the HSV1-TK gene and thereby trapped in cells and detected by nuclear imaging (107). Since other tissues also take up the imaging probe, high background emission from non-expression tissues decreases image contrast. Hence, the sensitivity of such methods is inherently lower than BLI where visible light is only emitted when the injected luciferin encounters luciferase in expressed tissues.

A nuclear reporter gene imaging approach has been reported recently for non-invasive imaging of beta cell islet grafts in NOD-SCID mice by Phelps, Kaufman, and coworkers (109). They transfected human islets with adenovirus-mediated gene transfer of a HSV1-TK mutant, HSV1-sr39tk. A CMV promoter was chosen to drive the sr39tk gene expression in islet cells rather than an insulin promoter that might be affected by blood glucose levels. The PET signal intensity of ^{18}F-FHBG directly correlated with islet mass ($r^2 = 0.739$, $P = 0.03$) as shown by analysis of PET images of human islets (1,000, 2,000, and 3,500 islets) implanted in axillary cavity of NOD-SCID mice. The diabetic mice that received 3,500 islets became euglycemic a few days after the implantation, indicating that human islet function was not significantly altered by the sr39tk gene transduction. The authors further longitudinally monitored the fate of rat islets implanted in liver by transfusing 1,500 – 2,000 islets into the mesenteric vein of diabetic NOD-SCID mice by microPET imaging with ^{18}F-FHBG. Interesting, it was found that the background uptake of ^{18}F-FHBG in the regions of head and chest was much higher in mice that received intrahepatic islets than in those that did not receive implants. The investigators attributed this observation to the metabolic imbalance associated with T1D and transient hyperglycemia in those animals. After subtracting the background signal, a 3-fold signal enhancement was observed in the liver region of animals that received islet implants at 4 days after transplantation in comparison with the same region of the animals without implanted islets. This signal enhancement dropped to 2-fold at 10 days after transplantation, and completely diminished at 40 days after transplantation. However, the mice remained euglycemic throughout the study period (50 days). As the imaging probe was cleared from the guts and kidneys, the microPET images reported showed spillover signals into the regions of interest. To overcome this problem, the investigators suggested using imaging probes with longer half-lives, e.g. ^{124}I-labeled FIAU (^{124}I: $t_{1/2} = 4.18$ d), so that imaging acquisition could be performed after the probe clears from non-target organs (109).

A number of compounds have been reported to have a specific binding affinity for beta cells such as the commonly prescribed sulfonylureas for the treatment of T2D (110). These compounds could potentially be developed as imaging probes for beta cells. However, to evaluate these compounds one by one in animal models or humans is a formidable and costly task. In light of the situation, Sweet and coworkers proposed a systematic *in vitro* screen method to select candidate compounds as potential beta cell imaging agents. Given the beta cell population in the pancreas, they set a criterion for potential imaging probe candidates with at least two orders of magnitude higher accumulation in beta cells *versus* in non-beta cells (111). For the systematic screening, they chose to use two beta cell types, INS-1 and rat islets. The former has a homogeneous cell population but the cells are not native, the latter contains not only the native beta cells but also non-beta cells in addition to diffusional tissue space. An exocrine pancreatic cell line, PANC-1, was used as a control. Two parameters were utilized to evaluate the specificity of candidate agents: cell uptake of radiolabeled candidate agents after a 30 min incubation period and radioactivity retention after a 40 min incubation period with radiolabel-free media. Eight compounds were screened using this methodology: glibenclamide, tolbutaime, serontin, L-DOPA, dopamine, nicotinamide, fluorodeoxyglucose,

and fluorodithizone. Whereas fluorodithizone showed the highest uptake in both rat islets and INS-1 cells, the highest beta cell binding specificity was exhibited by glibenclamide. However, uptake of glibenclamide in islets was only about 9 times that seen in PANC-1 cells in the absence of albumin. Interestingly, the specificity of dopamine was nearly as high as glibenclamide in rat islets but it became very low in INS-1 cells due to higher levels of secretory granules found in islets compared to beta cells. This feature of the pancreatic islets provides the basis of using ^{18}F-labeled DOPA to clinically diagnose two distinct forms of insulinism, a different beta cell abnormality, which we will discuss later. Although none of the compounds showed enough specificity to meet their preset criteria, two compounds with the highest specificity were selected for further *in vivo* evaluation in rats. Consistent with the authors' prediction, neither of the two compounds showed meaningful accumulation in the pancreas. To some extent, the result validated this systematic *in vitro* screening methodology for establishing guidelines for other researchers' studies.

As indicated above, a group of sulfonylureas are widely prescribed as antidiabetic agents for clinical treatment of T2D (110). They target a sulfonylurea receptor family with three known members: SUR1, SUR2A, and SUR2B. Of the three SUR receptors, SUR1 is overexpressed at the intracellular surface of the pancreatic beta cell plasma membrane but not in the exocrine pancreatic tissues (112–116). Therefore two commonly used sulfonylureas, glibenclamide and tolbutamide and their derivatives have been explored to develop specific beta cell imaging probes. Glibenclamide is named as glyburide in the United States.

Based on the parent structures of glibenclamide and tolbutamide, nearly two dozens of compounds or precursors have been designed, synthesized, and radiolabeled with ^{18}F or ^{11}C for PET imaging of the pancreatic beta cells by collaborations among the laboratories of Shiue, Schneider, and Schirrmacher in the United States and Germany. The lipophilicity (LogP), dissociation constants (K_d), half maximal inhibitory concentrations (IC_{50}), Hill coefficients, as well as insulin stimulation index of the new compounds have been measured and compared to those of the parent compounds (87,117–119). Based on *in vitro* results, two compounds, 2-^{18}F-fluoroethoxy-5-bromoglibenclamide and 2-^{18}F-fluoroethoxy-5-iodogliben-clamide, were evaluated in normal and diabetic mice (87) or normal rats (119). However, their accumulation in the pancreas was only marginally higher than in brain and pancreas accumulation was lower than the surrounding organs, such as kidneys, intestines, spleen, and blood (87,119). Furthermore, most of the injected doses of both compounds ended in liver without efficient hepatic clearance out to two hours post injection. Schneider and coworkers also made the first attempt to visualize the pancreatic beta cells with 2-^{18}F-fluoroethoxy-5-bromoglibenclamide in two healthy human subjects. Due to the approximately 10-fold higher relative uptake in the liver and slow washout from the blood, they were unable to visualize the pancreas (119). As the authors explained, the major reason for this failure could be attributed to avid binding of the compounds to plasma albumin. Indeed it was reported that nearly 99% of sulfonylureas in the blood is associated with albumin (120,121). In light of this problem, the authors proposed to increase the hydrophilicity of these compounds to reduce high uptake and retention in liver and blood. By replacing the fluoroethoxy functional group in 2-fluoroethoxy-5-bromo- glibenclamide with 2-(bis(carboxymethyl)amino)ethoxy, they synthesized a new glibenclamide compound that can be radiolabeled with either ^{99m}Tc or rhenium radioisotopes for SPECT imaging (119). Indeed, the ^{99m}Tc-labeled compound showed a 20-fold higher hydrophilicity as compared to the parent compound. It was evaluated in normoglycemic rats and, as expected, its uptake in liver and blood was more than three orders of magnitude lower than that of 2-^{18}F-fluoroethoxy-5-bromoglibenclamide. Although the pancreas uptake was also 10-fold lower, the contrast between the pancreas *versus* liver or the blood was significantly improved (119).

Repaglinide (Figure 4) is a non-sulfonylurea drug for the treatment of T2D, which also acts on SUR1. Due to its rapid *in vivo* kinetics and high binding affinity to SUR1, Schirrmacher and coworkers designed and synthesized two precursors in order to prepare ^{18}F-labeled and ^{11}C-labeled repaglinide (122,123) as potential beta cell imaging agents. Both PET tracers showed promising results *in vitro* but the have not been validated as PET imaging agents for beta cells to date.

The pancreas is an innervated peripheral organ with both parasympathetic and sympathetic neurons to tightly control its endocrine and exocrine functions. In fact, the pancreatic beta cells and neuroendocrine cells display many functional similarities and share a large number of gene products (124,125). This underlines a hypothesis that the neural imaging agents may find applications in beta cell imaging.

To date three successful attempts to employ neural imaging agents for beta cell imaging have been reported. This approach was first communicated by Clark and coworkers in 2003 (26). A radioligand that binds to the presynaptic vesicular acetylcholine transporter, 4-^{18}F-fluoro-benzyltrozamicol (FBT) (Figure 5), was used to scan four adult mice, two adult rhesus monkeys, and one adult human by PET. Impressively, the pancreas was clearly visualized in the PET images of all three mammals, which were dynamically scanned from 10 to 90 min post intravenous injection. The pancreas uptake of the PET tracer was persistently observed over the study period. While the liver was also shown in the images, the contrast measured by maximum standardized uptake values (SUV) for the pancreas *versus* liver was well above 1 in all scanned subjects. The mice exhibited the highest pancreas imaging contrast (mean 3.24; median: 3.02), followed by human (1.8) and rhesus monkeys (mean: 1.6; median: 1.7). It is noteworthy that all subjects in this study were normal mammals. To address the fact that the cholinergic innervation is reduced in T1D, and enhanced cholinergic activity may signal the onset of the disease (126,127), the authors suggested that this PET imaging probe could be used for diagnosis of diabetes in early stages (26). For T2D, the authors pointed out that neuroreceptor imaging may provide a useful way of evaluating some pancreatic disorders related to the changes of autonomic neural activity. Although this preliminary study showed potential of using neuroreceptor imaging agents to non-invasively assess the functions as well as the mass of beta cell islets, further studies using control and diabetic subjects and with larger sample sizes are needed.

As indicated before, L-DOPA (in a tritiated form) was among the compounds screened by Sweet and coworkers for potential beta cell imaging agent candidates (111). The relatively low *in vitro* beta cell binding specificity did not qualify this compound for further development as a PET imaging agent to assess the beta cell mass in diabetic patients. However, it was recently reported that ^{18}F-labeled L-DOPA can be used to non-invasively assess another type of biological abnormality of the pancreatic beta cells by PET (128–131), hyperinsulinism. In contrast to diabetes, hyperinsulinism is characterized by the hypersecretion of insulin which induces recurrent hypoglycemia during infancy causing severe neurological complications. Currently, a pancreatectomy must be carried out for the patients who are resistant to drug treatment (132–135). Hyperinsulinism appears in either a focal or a diffuse form with clinically indistinguishable patterns (132,135). The differential diagnosis of these two forms is of great importance because pancreatectomy procedures for the two forms are different. Currently, the diagnostic procedure is performed by pancreatic venous catheterization (PVS), which is technically difficult and invasive (136,137). Thus, it would be of great value to have a non-invasive imaging method using ^{18}F-fluoro-L-DOPA for accurate differential diagnosis.

The biochemical mechanism of the ^{18}F-fluoro-L-DOPA method can be attributed to the neuroendocrine nature of the pancreatic beta cells. Upon decarboxylation by the aromatic amino decarboxylase (AADC) in the pathological foci, ^{18}F-fluoro-L-DOPA is converted

to ^{18}F-dopamine, which in turn accumulates in the neurosecretory granules of the pancreatic neuroendocrine cells. This ^{18}F-fluoro-L-DOPA trapping mechanism has been partially verified by blocking the AADC enzyme, which results in back diffusion of the PET tracer from the neuroendocrine cells into extracellular spaces (128). As clearly shown in Figure 6, this ^{18}F-fluoro-L-DOPA PET method combined with MRI has been proven as an accurate and consistent diagnosis of focal and diffuse hyperinsulinism in three separate studies (128,130, 131) involving 15, 14, and 7 human patients, respectively.

The third successful example of using neural imaging agents for beta cell imaging employed ^{11}C-labeled dihydrotetrabenazine (DTBZ) (Figure 5) (47,48). Vesicular monoamine transporter type 2 (VMAT2) is expressed at dopamine nerve ends in the central nerve system (CNS) and in pancreatic beta cells but is absent in the exocrine tissues of the pancreas and many other abdominal tissues (138). Additionally, anti-VMAT2 and anti-insulin antibodies have been shown to co-localize in beta cell islets (139–141). The specific binding affinity of DTBZ to the beta cell islet membrane was first evaluated by incubating tritiated DTBZ with total membrane proteins prepared from purified human islets and purified exocrine pancreas tissue. The tritiated DTBZ ligand bound exclusively to the human islet membrane but not to the exocrine pancreas (138).

The first *in vivo* biodistribution experiment with ^{11}C-labeled DTBZ was performed in normal rats in 1994 (142). Although the pancreas showed the highest uptake among the harvested organs including the liver, spleen, kidney, and stomach at 15 – 60 min post injection, ^{11}C-labeled DTBZ had not been considered for beta cell imaging until recently. In contrast, this PET tracer has been used as a specific ligand for VMAT2 in clinical PET imaging of the CNS since 1995 (143).

Recently Harris and coworkers reported longitudinal PET imaging studies with ^{11}C-labeled DTBZ in seven BB-DP rats (47,48). The animals were scanned three times during the study period at ages 7 weeks, 8 – 9 weeks, and 11 – 12 weeks, respectively. In the first and second scans, all animals were euglycemic. Pancreatic uptake was measured by max SUV values, which significantly dropped over time of study. The positively correlated relationship between the max SUV values and age ($r^2 = 0.58$) was believed to reflect the progress of diabetes in the animals. The area under the curve of the intraperiotoneal serum insulin concentrations (AUC IPGTT) was used as an index of glycemic control. It was found that these index measurements significantly correlated with pancreatic uptake of ^{11}C-labeled DTBZ by a hyperbolic function. Furthermore, using histomorphometry and RT-PCR assays, it was found that the decrease in pancreatic uptake of DTBZ over time was in agreement with loss of beta cells and the decline of VMAT2 expression levels as the disease was progressing (47,48). However, the usefulness of this PET imaging agent has not yet been addressed in diabetic humans.

Cell membrane receptor specific monoclonal antibodies and peptides have long been used as targeting molecules for cancer diagnosis and therapy (144,145). Compared to monoclonal antibodies, peptides have more efficient tissue penetration and rapid clearance from non-target organs, and normally are not immunogenic upon repetitive administration. Currently the problems associated with proteolytic peptide degradation can be largely overcome by using D-amino acids, sequence cyclization, and/or modification of the N- or C-terminal amino acids (144,145). In spite of the success of using peptides for cancer, to the best of our knowledge, peptides have not been reported as imaging agents for the non-invasive assessment of beta cell islets.

By panning a random phage-displayed 20-mer peptide library on freshly isolated rat islets, the Brown laboratory recently obtained two peptide phage clones (termed as RIP1 and RIP2) that bind to islets *ex vivo* (146). In an *in vitro* binding assay using the INS-1 derived beta cell line,

832/13 (147), which displays robust glucose stimulated insulin secretion, the RIP1 phage clone displayed 8-fold higher beta cell uptake compared to the RIP2 phage, indicating that the RIP1 phage homes to beta cells while the RIP2 phage may bind to other cell types in islets. To test the *in vivo* beta cell binding of these phage clones, RIP1, RIP2, and a control phage clone containing a random peptide sequence were evaluated in both Sprague-Dawley rats and Zucker diabetic fatty rats (a T2D animal model) by the jugular vein injection. The phage clones were allowed to circulate in the animals for 2 h and after the animals were sacrificed, the harvested organs were stained with an anti-phage antibody to visualize the presence of phage. As shown in Figure 7, the RIP1 phage is clearly visible in rat islets and the image concurs with insulin expression stained with an anti-insulin antibody. This suggests that the RIP1 phage preferentially binds to beta cells. Impressively, the RIP1 phage did not show significant accumulation in the pancreatic islets of the T2D diabetic rat, suggesting that it can differentiate between functional and dysfunctional beta cells.

To explore the potential application of the RIP1 phage clone and its targeting peptide sequence as nuclear imaging agents for non-invasive beta cell mass and/or function assessment, we have preliminary evaluated the RIP1 phage clone by radiolabeling it with ^{125}I and with ^{124}I ($t_{1/2}$: 4.18 d; β^+: 23%) for *in vitro* and *in vivo* studies. A control phage with random peptide sequence was used for comparison. Both RIP1 and control phage clones were labeled with ^{125}I and ^{124}I at radiochemical yields of 30 – 40%. The highest achievable specific activity was 5×10^{-5} μCi/cfu. Analyzed by radio-ITLC, greater than 95% radiochemical purity was obtained for the ^{125}I or ^{124}I labeled phage clones after separation and purification.

In vitro assays were performed on both freshly isolated rat islets and INS 832/13 cells. Islets were isolated from the pancreas of Sprague-Dawley rats weighing 150–175 g and embedded into alginate beads (ϕ 2.5-mm). The ^{125}I-labeled phage clones were then added (n = 5 for each phage) and the mixture was incubated at 37°C for 30 min, after which the beads were washed three times by cold PBS (10 mM). Phage binding was determined by a gamma counter. For studies using the insulinoma cells, 1×10^7 cfu of each ^{125}I labeled phage clone (0.4 – 0.7 μCi) was incubated with 1×10^6 INS 832/13 cells (six wells per phage) in a 12-well plate at 37°C. After 30 min, the cells were washed by cold PBS three times and imaged by a Cyclone autoradiography system (Perkin Elmer). After the imaging, the cells were harvested and counted using a gamma counter. As shown in Figure 8, the number of RIP 1 phage attached to rat islets embedded in beads was significantly higher than that of the control phage (RIP1: $(3.16 \pm 1.17) \times 10^5$ cfu/bead; Control: $(0.95 \pm 0.35) \times 10^5$ cfu/bead. $p < 0.005$).

Because the pancreatic islets represent a mixture of cells, the two ^{125}I labeled phage clones were further tested on INS 832/13 beta cells. As shown in Figure 9 (lower panel), 3-fold greater uptake of phage in the beta cells was observed for the RIP1 phage compared to the control phage. Consistent with this finding, cells incubated the RIP1 phage showed significantly higher signal intensity by autoradiography than cells incubated with control phage (Figure 9, upper panel).

In vivo biodistribution studies of the two ^{125}I labeled phage clones were carried out in normal male Sprague-Dawley rats at the age of 4–5 weeks weighing 150–175 g. Each animal received 5 μCi of ^{125}I labeled phage clone *via* tail vein infusion and were subsequently sacrificed at 1, 4, 24 and 48 h post injection (n = 4 at each time point). Organs of interest were removed, weighed and counted. Standards were prepared and counted along with the samples to calculate the percent injected dose per gram (%ID/g).

As shown in Figure 10, uptake of ^{125}I-labeled RIP1 phage by the pancreas was significantly higher than that of ^{125}I-labeled control phage at 4 h p.i. (RIP1: 0.35 ± 0.08 %ID/g; Control: 0.17 ± 0.05 %ID/g. $p < 0.01$). Considering the phage size, it was surprising to see low uptake

of both phage clones in liver (RIP1: 1.14 ± 0.55 %ID/g; Control: 0.93 ± 0.19 %ID/g at 4 h p.i.) and rather efficient overall clearance (RIP1 and Control: > 80%ID was excreted within 24 h p.i.). Both phage clones were rapidly cleared from the blood stream (RIP1: 0.56 ± 0.05 %ID/g at 1-h p.i., 0.37 ± 0.08 %ID/g at 4-h p.i., and 0.04 ± 0.00 %ID/g at 24-h p.i.; Control: 0.34 ± 0.03 %ID/g at 1-h p.i., 0.32 ± 0.75 %ID/g at 4-h p.i., and 0.03 ± 0.01 %ID/g at 24-h p.i.). Impressively, at 4 h p.i., the RIP1 phage showed significantly lower accumulation in both the spleen (RIP1: 1.41 ± 0.29 %ID/g; Control: 5.30 ± 0.96 %ID/g. $p < 0.001$) and the kidneys (RIP1: 0.45 ± 0.04 %ID/g; Control: 1.21 ± 0.14 %ID/g. $p < 0.001$) than that of the control phage.

Because the RIP1 phage demonstrated elevated uptake in the pancreas, lower accumulation in the spleen and the kidneys, and efficient clearance from major organs in the biodistribution studies in normal rats, we set out to image the pancreas with ^{124}I-labeled RIP1 phage in normal rats. Sprague-Dawley rats were injected with the two ^{124}I-labeled phage clones *via* the tail vein (640 – 683 μCi of 1×10^9 cfu) and imaged using a home-built small animal PET system (148) at 4 h p.i. As shown in Figure 11, with ^{124}I-labeled RIP1 phage, a bright area between the stomach and the liver is clearly visible. However, limited by the sensitivity of our small animal PET system and the capability of our in-house developed image reconstruction software (148,149), we could not identify with certainty whether the intense areas reflect the pancreas or other abdominal organs. To answer this question definitely we performed a post-PET biodistribution study of rats after imaging. The ratios between the uptake values (%ID/g) of the ^{124}I-labeled RIP1 phage in the pancreas and other organs are 16.2 (pancreas/brain), 6.3 (pancreas/fat), 5.9 (pancreas/muscle), 1.4 (pancreas/kidney), 1.3 (pancreas/liver), 0.6 (pancreas/stomach), and 0.3 (pancreas/spleen). Therefore, the bright region between the stomach and the liver in Figure 11 very likely reflects the pancreas. Further evaluations of this RIP1 phage are under investigation.

Taken together, our preliminary data show that the RIP1 phage preferentially accumulates in the pancreas. Considering a previous report on this phage (146), we conclude that the elevated pancreas uptake of the $^{125/124}$I labeled RIP1 phage is likely caused by its specific beta cell binding. The $^{125/124}$I labeled RIP1 phage clones also showed high uptake in the stomach. This is likely due to the endogenous sodium iodide symporter (NIS) expression in the stomach which absorbs an extra amount of $^{125/124}$I radioactivity in the form of free iodide because of the deiodination of the radiolabeled phage.

Although both phage clones showed relatively efficient clearance from the animals, they have inherently tendency to accumulate in the organs of the reticuloendothelial system (RES), such as the liver and spleen, simply due to the phage particle size. Considering these factors, we plan to use the RIP1 peptide sequence for the further development of beta cell imaging agents. The Brown laboratory has recently designed and reported a unique scaffold constructed from a branched lysine core to present multiple copies of targeting peptides on the end of polyethylene glycol (PEG) chains (150–156). For cell-specific delivery of payloads, such as drug, imaging probes, and genes, a cysteine handle is introduced to the construct for payload attachment. In fact, the design of such a scaffold was partially intended to mimic the multimeric fashion of the peptides presented on the tip of the M13 phage clones in phage display. A typical tetrameric peptide construct is shown in Figure 12.

To avoid excess stomach uptake seen in the radioiodine experiments, this radioisotope will be avoided in future radiochemistry procedures. To date, we have designed and synthesized several maleimide derivatives as precursors to radiolabel the cysteine-containing peptide constructs with ^{18}F, ^{64}Cu, ^{99m}Tc, or ^{111}In for PET and SPECT imaging of the pancreatic beta cells.

4. CONCLUSIONS

In summary, there is a growing need to develop early diagnostic methods for the non-invasive assessment of the pancreatic beta cells as T1D and T2D and other beta cell associated metabolic diseases are becoming epidemic. Newly developed imaging agents will aid in the mechanistic understanding of the progression of beta cell disease as well as being translated into the clinic for early diagnosis. Among the current imaging methods, MRI provides images with the highest resolution. Aided by SPIO as a T2 contrast agent, MRI has been successfully applied to monitor the mass change of transplanted beta cell islets for the treatment of T1D. Other alternative ways, such as using responsive Mn-enhanced or PARACEST MRI contrast agents, have also shown potential in the assessment of the pancreatic beta cells. Due to insufficient deep tissue penetration, optical imaging techniques are currently confined to small animal studies although BLI has shown promising results for non-invasive assessment of the fate of transplanted pancreatic islets. Successful PET imaging of the normal pancreas in three mammalian species with ^{18}F-labeled FBT, the diabetic pancreas in rats with ^{11}C-labeled DTBZ, and the clinical differentiation of focal and diffuse hyperinsulinism with ^{18}F-labeled L-DOPA, nuclear imaging methods have great momentum to move forward the molecular imaging of the pancreatic beta cell islets.

With the superior inherent sensitivity, the role of nuclear imaging techniques is mainly defined by the successful development of radiotracers that can specifically target the pancreatic beta cells. Based on the neuroendocrine nature of the pancreatic beta cell islets, it appears straightforward to systematically screen the current existing neuroimaging agents for such beta cell islet specific nuclear imaging probes. In addition, our preliminary data have shown that peptide sequences selected by panning random phage-displayed peptide libraries on freshly isolated islets also have potential.

Supplementary Material

Refer to Web version on PubMed Central for supplementary material.

Acknowledgments

This work was partially supported by a Program Project Grant from the National Institutes of Health (PO1 DK058398).

REFERENCES

1. National Diabetes Fact Sheet, the American Diabetes Association. https://www.diabetes.org/diabetes-statistics.jsp
2. Kim MS, Polychronakos C. Immunogenetics of Type 1 Diabetes. Hormone Research 2005;64:180–188. [PubMed: 16254432]
3. Steele C, Hagopian WA, Gitelman S, Masharani U, Cavaghan M, Rother KI, Donaldson D, Harlan DM, Bluestone J, Herold KC. Insulin Secretion in Type 1 Diabetes. Diabetes 2004;53:426–433. [PubMed: 14747294]
4. Dwarakanathan A. Diabetes update. J Insur Med 2006;38:20–30. [PubMed: 16642640]
5. Rolandsson O, Hagg E, Hampe C, Sullivan EP Jr, Nilsson M, Jansson G, Hallmans G, Lernmark A. Glutamate decarboxylase (GAD65) and tyrosine phosphatase-like protein (IA-2) autoantibodies index in a regional population is related to glucose intolerance and body mass index. Diabetologia 1999;42:555–559. [PubMed: 10333047]
6. Ko IY, Ihm SH, Yoon JW. Studies on autoimmunity for initiation of beta-cell destruction. VIII. Pancreatic beta-cell dependent autoantibody to a 38 kilodalton protein precedes the clinical onset of diabetes in BB rats. Diabetologia 1991;34:548–554. [PubMed: 1936657]
7. Barnett AH, Eff C, Leslie RDG, Pyke DA. Diabetes in identical twins. A study of 200 pairs. Diabetologia 1981;20:87–93. [PubMed: 7193616]

8. Jun H-S, Yoon J-W. A new look at viruses in type 1 diabetes. Diabetes Metab Res Rev 2003;19:8–31. [PubMed: 12592641]
9. DeFronzo RA, Deibert D, Hendler R, Felig P, Soman V. Insulin sensitivity and insulin binding to monocytes in maturity-onset diabetes. J Clin Invest 1979;63:939–946. [PubMed: 376552]
10. DeFronzo RA. The triumvirate: b-cell, muscle, liver: a collusion responsible for NIDDM. Diabetes 1988;37:667–687. [PubMed: 3289989]
11. Beck-Nielsen H. The pathogenic role of an insulin-receptor defect in diabetes mellitus of the obese. Diabetes 1978;27:1175–1181. [PubMed: 720772]
12. Olefsky JM, Reaven GM. Decreased insulin binding to lymphocytes from diabetic subjects. J Clin Invest 1974;54:1323–1328. [PubMed: 4474186]
13. Freidenberg GR, Henry RR, Klein HH, Reichart DR, Olefsky JM. Decreased kinase activity of insulin receptors from adipocytes of non-insulindependent diabetic subjects. J Clin Invest 1987;79:240–250. [PubMed: 3540010]
14. Maegawa H, Shigeta Y, Egawa K, Kobayashi M. Impaired autophosphorylation of insulin receptors from abdominal skeletal muscles in nonobese subjects with NIDDM. Diabetes 1991;40:815–819. [PubMed: 1647993]
15. Golay A, DeFronzo RA, Ferrannini E. Oxidative and non-oxidative glucose metabolism in non-obese type 2 (non-insulin-dependent) diabetic patients. Diabetologia 1988;31:585–591. [PubMed: 3065112]
16. Golay A, Felber JP, Jequier E, DeFronzo RA, Ferrannini E. Metabolic basis of obesity and noninsulin-dependent diabetes mellitus. Diabetes Metab Rev 1988;4:727. [PubMed: 3069401]
17. Ciaraldi TP, Kolterman OG, Scarlett JA, Kao M, Olefsky JM. Role of glucose transport in the postreceptor defect of non-insulin-dependent diabetes mellitus. Diabetes 1982;31:1016–1022. [PubMed: 6757010]
18. Handberg A, Vaag A, Damsbo P, Beck-Nielsen H, Vinten J. Expression of insulin regulatable glucose transporters in skeletal muscle from type 2 (noninsulin-dependent) diabetic patients. Diabetologia 1990;33:625. [PubMed: 2258000]
19. Vaag A, Henriksen JE, Beck-Nielsen H. Decreased insulin activation of glycogen synthase in skeletal muscles in young nonobese Caucasian firstdegree relatives of patients with non-insulin-dependent diabetes mellitus. Diabetes 1992;89:782–788.
20. Groop LC, Kankuri M, Schalin-Jäntti C. Association between polymorphism of the glycogen synthase gene and non-insulin-dependent diabetes mellitus. N Engl J Med 1993;328:10. [PubMed: 8416266]
21. Taylor SI. Molecular mechanisms of insulin resistance: lessons from patients with mutations in the insulin-receptor gene. Diabetes 1992;41:1473–1490. [PubMed: 1327927]
22. Laughlin MR. Why Imaging the Pancreatic Beta Cell? Curr Med Chem 2004;4:251–252.
23. Paty BW, Bonner-Weir S, Laughlin MR, McEwan AJ, Shapiro AM. Toward development of imaging modalities for islets after transplantation: insights from the National Institutes of Health Workshop on Beta Cell Imaging. Transplantation 2004;77:1133–1137. [PubMed: 15114073]
24. Moore A, Bonner-Weir S, Weissleder R. Noninvasive in vivo measurement of beta-cell mass in mouse model of diabetes. Diabetes 2001;50:2231–2236. [PubMed: 11574403]
25. Moore A, Sun PZ, Ho¨gemann DC, Weissleder R, Lipes MA. MRI of Insulitis in Autoimmune Diabetes. Magnetic Resonance in Medicine 2002;47:751–758. [PubMed: 11948737]
26. Clark PB, Gage HD, Brown-Proctor C, Buchheimer N, Calles-Escandon J, Mach RH, Morton KA. Neurofunctional imaging of the pancreas utilizing the cholinergic PET radioligand [^{18}F]4-fluorobenzyltrozamicol. Eur J Nucl Med Mol Imaging 2003;31:258–260. [PubMed: 15129709]
27. Achilefu S. Optical Imaging Agents and Potential Application in the Assessment of Pancreatic Beta Cells. Curr Med Chem 2004;4:253–269.
28. Alavi A, Kung JW, Zhuang H. Implications of PET based molecular imaging on the current and future practice of medicine. Semin Nucl Med 2004;34:56–69. [PubMed: 14735459]
29. Chen X, Kaufman DB. Bioluminescence Imaging of Pancreatic Islet Transplants. Curr Med Chem 2004;4:301–308.
30. Jira´k D, Krı´z J, Herynek Vt, Andersson B, Girman P, Burian M, Saudek Fe, Ha´jek M. MRI of Transplanted Pancreatic Islets. Magnetic Resonance in Medicine. 2004

31. Kohler M, Nyqvist D, Moede T, Wahlstedt H, Cabrera O, Leibiger I, Berggren P-O. Imaging of Pancreatic Beta-Cell Signal-Transduction. Curr Med Chem 2004;4:281–299.
32. Madsen OD, Kaestner DB. Antibodies to Islet Beta Cell Surface Markers. Curr Med Chem 2004;4:309–311.
33. Moore A, Grimm J, Han B, Santamaria P. Tracking the recruitment of diabetogenic CD8+ T-cells to the pancreas in real time. Diabetes 2004;53:1459–1466. [PubMed: 15161749]
34. Moore A, Medarova ED. Approaches for Imaging the Diabetic Pancreas: First Results. Curr Med Chem 2004;4:315–331.
35. Philipson LH, Roe MW. Imaging Metabolic and Signaling Tragets in the Pancreatic Beta Cells. Curr Med Chem 2004;4:333–337.
36. Powers AC, Jansen ED. In Vivo Bioluminescence Imaging to Assess Pancreatic Islets. Curr Med Chem 2004;4:339–347.
37. Sweet IR, Cook DL, Lernmark A, Greenbaum CJ, Krohn KA. Non-invasive imaging of beta cell mass: a quantitative analysis. Diabetes Technol Ther 2004;6:652–659. [PubMed: 15628819]
38. Woods M, Zhang S, Sherry AD. Toward the Design of MR Agents for Imaging Beta-cell Function. Curr Med Chem 2004;4:349–369.
39. Koblas T, Girman P, Berkova Z, Jirak D, Kriz J, Dovolilova E, Zacharovova K, Hajek M, Saudek F. Magnetic Resonance Imaging of Intrahepatically Transplanted Islets Using Paramagnetic Beads. Transplantation Proceedings 2005;37:3493–3495. [PubMed: 16298639]
40. Kriz J, Jira´k D, Girman P, Berkova´ Z, Zacharovova K, Honsova E, Lodererova A, Hajek M, Saudek F. Magnetic Resonance Imaging of Pancreatic Islets in Tolerance and Rejection. Transplantation 2005;80:1596–1603. [PubMed: 16371931]
41. Malaisse WJ. Non-invasive imaging of the endocrine pancreas (review). Int J Mol Med 2005;15:243–246. [PubMed: 15647838]
42. Schneider S, Feilen PJ, Schreckenberger M, Schwanstecher M, Schwanstecher C, Buchholz HG, Thews O, Oberholzer K, Korobeynikov A, Bauman A, Comagic S, Piel M, Schirrmacher E, Shiue CY, Alavi AA, Bartenstein P, Rösch F, Weber MM, Klein HH, Schirrmacher R. In Vitro and In Vivo Evaluation of Novel Glibenclamide Derivatives as Imaging Agents for the Non-Invasive Assessment of the Pancreatic Islet Cell Mass in Animals and Humans. Exp Clin Endocrinol Diabetes 2005;113:388–395. [PubMed: 16025400]
43. Evgenov NV, Medarova Z, Pratt J, Pantazopoulos P, Leyting S, Bonner-Weir S, Moore A. In vivo imaging of immune rejection in transplanted pancreatic islets. Diabetes 2006;55:2419–2428. [PubMed: 16936189]
44. Gimi B, Leoni L, Oberholzer J, Braun M, Avila J, Wang Y, Desai T, Philipson LH, Magin RL, Roman BB. Functional MR microimaging of pancreatic beta-cell activation. Cell Transplant 2006;15:195–203. [PubMed: 16719054]
45. Nagamatsu S, Ohara-Imaizumi M, Nakamichi Y, Kikuta T, Nishiwaki C. Imaging docking and fusion of insulin granules induced by antidiabetes agents: sulfonylurea and glinide drugs preferentially mediate the fusion of newcomer, but not previously docked, insulin granules. Diabetes 2006;55:2819–2825. [PubMed: 17003348]
46. Roth DJ, Jansen ED, Powers AC, Wang TG. A novel method of monitoring response to islet transplantation: bioluminescent imaging of an NF-kB transgenic mouse model. Transplantation 2006;81:1185–1190. [PubMed: 16641606]
47. Souza F, Freeby M, Hultman K, Simpson N, Herron A, Witkowsky P, Liu E, Maffei A, Harris PE. Current progress in non-invasive imaging of beta cell mass of the endocrine pancreas. Curr Med Chem 2006;13:2761–2773. [PubMed: 17073627]
48. Souza F, Simpson N, Raffo A, Saxena C, Maffei A, Hardy M, Kilbourn M, Goland R, Leibel R, Mann JJ, Van Heertum R, Harris PE. Longitudinal noninvasive PET-based beta cell mass estimates in a spontaneous diabetes rat model. J Clin Invest 2006;116:1506–1513. [PubMed: 16710474]
49. Tai JH, Foster P, Rosales A, Feng B, Hasilo C, Martinez V, Ramadan S, Snir J, Melling CW, Dhanvantari S, Rutt B, White DJ. Imaging islets labeled with magnetic nanoparticles at 1.5 Tesla. Diabetes 2006;55:2931–2938. [PubMed: 17065328]

50. Ward KM, Aletras AH, Balaban RS. A new class of contrast agents for MRI based on proton chemical exchange dependent saturation transfer (CEST). J Magn Reson 2000;143:79–87. [PubMed: 10698648]
51. Ward KM, Balaban RS. Determination of pH using water protons and chemical exchange dependent saturation transfer (CEST). Magn Reson Med 2000;44:799–802. [PubMed: 11064415]
52. Zhang S, Kovacs Z, Burgess S, Aime S, Terreno E, Sherry AD. [DOTA-bis(amide)]lanthanide complexes: NMR evidence for differences in water-molecule exchange rates for coordination isomers. Chemistry 2001;7:288–296. [PubMed: 11205022]
53. Zhang S, Winter P, Wu K, Sherry AD. A novel europium(III)-based MRI contrast agent. J Am Chem Soc 2001;123:1517–1518. [PubMed: 11456734]
54. Zhang S, Wu K, Sherry AD. Gd3+ complexes with slowly exchanging bound-water molecules may offer advantages in the design of responsive MR agents. Invest Radiol 2001;36:82–86. [PubMed: 11224755]
55. Aime S, Barge A, Batsanov AS, Botta M, Castelli DD, Fedeli F, Mortillaro A, Parker D, Puschmann H. Controlling the variation of axial water exchange rates in macrocyclic lanthanide(III) complexes. Chem Commun (Camb) 2002:1120–1121. [PubMed: 12122694]
56. Aime S, Barge A, Delli Castelli D, Fedeli F, Mortillaro A, Nielsen FU, Terreno E. Paramagnetic lanthanide(III) complexes as pH-sensitive chemical exchange saturation transfer (CEST) contrast agents for MRI applications. Magn Reson Med 2002;47:639–648. [PubMed: 11948724]
57. Aime S, Delli Castelli D, Fedeli F, Terreno E. A paramagnetic MRI-CEST agent responsive to lactate concentration. J Am Chem Soc 2002;124:9364–9365. [PubMed: 12167018]
58. Aime S, Delli Castelli D, Terreno E. Novel pH-reporter MRI contrast agents. Angew Chem Int Ed Engl 2002;41:4334–4336. [PubMed: 12434381]
59. Aime S, Delli Castelli D, Terreno E. Supramolecular adducts between poly-L-arginine and [TmIIIdotp]: a route to sensitivity-enhanced magnetic resonance imaging-chemical exchange saturation transfer agents. Angew Chem Int Ed Engl 2003;42:4527–4529. [PubMed: 14520757]
60. Zhang S, Merritt M, Woessner DE, Lenkinski RE, Sherry AD. PARACEST agents: modulating MRI contrast via water proton exchange. Acc Chem Res 2003;36:783–790. [PubMed: 14567712]
61. Zhang S, Trokowski R, Sherry AD. A paramagnetic CEST agent for imaging glucose by MRI. J Am Chem Soc 2003;125:15288–15289. [PubMed: 14664562]
62. Aime S, Carrera C, Delli Castelli D, Geninatti Crich S, Terreno E. Tunable imaging of cells labeled with MRI-PARACEST agents. Angew Chem Int Ed Engl 2005;44:1813–1815. [PubMed: 15723362]
63. Aime S, Delli Castelli D, Terreno E. Highly sensitive MRI chemical exchange saturation transfer agents using liposomes. Angew Chem Int Ed Engl 2005;44:5513–5515. [PubMed: 16052647]
64. Terreno E, Botta M, Boniforte P, Bracco C, Milone L, Mondino B, Uggeri F, Aime S. A multinuclear NMR relaxometry study of ternary adducts formed between heptadentate Gd(III) chelates and L-lactate. Chemistry 2005;11:5531–5537. [PubMed: 16013030]
65. Aime S, Fedeli F, Sanino A, Terreno E. A R2/R1 ratiometric procedure for a concentration-independent, pH-responsive, Gd(III)-based MRI agent. J Am Chem Soc 2006;128:11326–11327. [PubMed: 16939235]
66. Terreno E, Botta M, Dastru W, Aime S. Gd-enhanced MR images of substrates other than water. Contrast Media Mol Imaging 2006;1:101–105. [PubMed: 17193685]
67. Brissova M, Fowler MJ, Nicholson WE, Chu A, Hirshberg B, Harlan DM, Powers AC. Assessment of human pancreatic islet architecture and composition by laser scanning confocal microscopy. J Histochem Cytochem 2005;53:1087–1097. [PubMed: 15923354]
68. Watkins S, Geng X, Li L, Papworth G, Robbins PD, Drain P. Imaging secretory vesicles by fluorescent protein insertion in propeptide rather than mature secreted peptide. Traffic 2002;3:461–471. [PubMed: 12047554]
69. Bennett BD, Jetton TL, Ying G, Magnuson MA, Piston DW. Quantitative subcellular imaging of glucose metabolism within intact pancreatic islets. J Biol Chem 1996;271:3647–3651. [PubMed: 8631975]
70. Ben-Yehudah A, Reinhart B, Navara C, Kotzuk J, Witchel S, Schatten G, Chaillet JR. Specific dynamic and noninvasive labeling of pancreatic beta cells in reporter mice. Genesis 2005;43:166–174. [PubMed: 16283623]

71. Chen X, Zhang X, Larson CS, Baker MS, Kaufman DB. In vivo bioluminescence imaging of transplanted islets and early detection of graft rejection. Transplantation 2006;81:1421–1427. [PubMed: 16732180]
72. Bertera S, Geng X, Tawadrous Z, Bottino R, Balamurugan AN, Rudert WA, Drain P, Watkins SC, Trucco M. Body window-enabled in vivo multicolor imaging of transplanted mouse islets expressing an insulin-Timer fusion protein. Biotechniques 2003;35:718–722. [PubMed: 14579736]
73. Fowler M, Virostko J, Chen Z, Poffenberger G, Radhika A, Brissova M, Shiota M, Nicholson WE, Shi Y, Hirshberg B, Harlan DM, Jansen ED, Powers AC. Assessment of pancreatic islet mass after islet transplantation using in vivo bioluminescence imaging. Transplantation 2005;79:768–776. [PubMed: 15818318]
74. Virostko J, Chen Z, Fowler M, Poffenberger G, Powers AC, Jansen ED. Factors influencing quantification of in vivo bioluminescence imaging: application to assessment of pancreatic islet transplants. Mol Imaging 2004;3:333–342. [PubMed: 15802050]
75. Lu Y, Dang H, Middleton B, Zhang Z, Washburn L, Campbell-Thompson M, Atkinson MA, Gambhir SS, Tian J, Kaufman DL. Bioluminescent monitoring of islet graft survival after transplantation. Mol Ther 2004;9:428–435. [PubMed: 15006610]
76. Park SY, Wang X, Chen Z, Powers AC, Magnuson MA, Head WS, Piston DW, Bell GI. Optical imaging of pancreatic beta cells in living mice expressing a mouse insulin I promoter-firefly luciferase transgene. Genesis 2005;43:80–86. [PubMed: 16108006]
77. Medarova Z, Bonner-Weir S, Lipes M, Moore A. Imaging beta-cell death with a near-infrared probe. Diabetes 2005;54:1780–1788. [PubMed: 15919800]
78. Evgenov NV, Medarova Z, Dai G, Bonner-Weir S, Moore A. In vivo imaging of islet transplantation. Nat Med 2006;12:144–148. [PubMed: 16380717]
79. Like AA, Gerritsen GC, Dulin WE, Gaudreau P. Studies in the diabetic Chinese hamster: electron microscopy of pancreatic islets. Diabetologia 1974;10:509–520. [PubMed: 4615024]
80. Malaisse WJ, Like AA, Malaisse-Lagae F, Gleason RE, Soeldner JS. Insulin secretion in vitro by the pancreas of the sand rat (Psammomys obesus). Diabetes 1968;17:754–759. [PubMed: 4881994]
81. Orci L, Amherdt M, Malaisse-Lagae F, Perrelet A, Dulin WE, Gerritsen GC, Malassie WJ, Renold AE. Morphological characterization of membrane systems in A- and B-cells of the Chinese hamster. Diabetologia 1974;10:529–539. [PubMed: 4217292]
82. Malaisse WJ, Damhaut P, Ladriere L, Goldman S. Fate of 2-deoxy-2-[18F]fluoro-D-glucose in hyperglycemic rats. Int J Mol Med 2000;6:549–552. [PubMed: 11029522]
83. Malaisse WJ, Damhaut P, Malaisse-Lagae F, Ladriere L, Olivares E, Goldman S. Fate of 2-deoxy-2-[18F]fluoro-D-glucose in control and diabetic rats. Int J Mol Med 2000;5:525–532. [PubMed: 10762657]
84. Malaisse WJ. On the track to the beta-cell. Diabetologia 2001;44:393–406. [PubMed: 11357468]
85. Malaisse WJ, Doherty M, Kadiata MM, Ladriere L, Malaisse-Lagae F. Pancreatic fate of D-[3H] mannoheptulose. Cell Biochem Funct 2001;19:171–179. [PubMed: 11494306]
86. Malaisse WJ, Ladriere L. Assessment of B-cell mass in isolated islets exposed to D-[3H] mannoheptulose. Int J Mol Med 2001;7:405–406. [PubMed: 11254882]
87. Shiue C-Y, Schmitz A, Schirrmacher R, Shiue GG, Alavi A. Potential Approaches for Beta Cell Imaging with PET and SPECT. Curr Med Chem 2004;4:271–280.
88. Courtois P, Sener A, Malaisse WJ. Effects of D-mannoheptose and D-glycero-D-gulo-heptose upon D-glucose metabolism and insulinotropic action in rat pancreatic islets and D-glucose phosphorylation by hexokinase isoenzymes: comparison with D-mannoheptulose. Int J Mol Med 2000;6:171–175. [PubMed: 10891561]
89. Giroix MH, Scruel O, Courtois P, Sener A, Portha B, Malaisse WJ. Comparison between D-[3-3H]- and D-[5-3H]glucose and fructose utilization in pancreatic islets from control and hereditarily diabetic rats. Arch Biochem Biophys 2002;408:111–123. [PubMed: 12485609]
90. Malaisse WJ, Zhang Y, Jijakli H, Courtois P, Sener A. Metabolism of D-glucose anomers in rat pancreatic islets exposed to equilibrated D-glucose. Horm Metab Res 2004;36:281–285. [PubMed: 15156406]
91. Ramirez R, Courtois P, Ladriere L, Kadiata MM, Sener A, Malaisse WJ. Uptake of D-mannoheptulose by rat erythrocytes, hepatocytes and parotid cells. Int J Mol Med 2001;8:37–42. [PubMed: 11408946]

92. Sener A, Bessieres B, Courtois P, Ladriere L, Louchami K, Jijakli H, Malaisse WJ. Uptake of 1-deoxy-1-[125I]iodo-D-mannoheptulose by different cell types: in vitro and in vivo experiments. Int J Mol Med 2001;7:495–500. [PubMed: 11295110]

93. Zhang HX, Jijakli H, Courtois P, Sener A, Malaisse WJ. Labelling of lipids by D-[1-14C]glucose, D-[6-14C] glucose and D-[3-3H]glucose in pancreatic islets from normal and GK rats. Mol Cell Biochem 2003;252:247–251. [PubMed: 14577599]

94. Zhang Y, Courtois P, Sener A, Malaisse WJ. Dissimilar effects of D-mannoheptulose on the phosphorylation of alpha- versus beta-D-glucose by either hexokinase or glucokinase. Int J Mol Med 2004;14:107–112. [PubMed: 15202024]

95. Zhang Y, Courtois P, Sener A, Malaisse WJ. Anomeric specificity of D-[U-14C]glucose incorporation into glycogen in rat hemidiaphragms. Biochimie 2004;86:913–918. [PubMed: 15667941]

96. Crenier L, Courtois P, Malaisse WJ. Uptake of tritiated D-mannoheptulose by liver, pancreatic exocrine and endocrine cells. Int J Mol Med 2001;8:155–157. [PubMed: 11445866]

97. Ladriere L, Malaisse-Lagae F, Alejandro R, Malaisse WJ. Pancreatic fate of a (125)I-labelled mouse monoclonal antibody directed against pancreatic B-cell surface ganglioside(s) in control and diabetic rats. Cell Biochem Funct 2001;19:107–115. [PubMed: 11335935]

98. Hampe CS, Wallen AR, Schlosser M, Ziegler M, Sweet IR. Quantitative evaluation of a monoclonal antibody and its fragment as potential markers for pancreatic beta cell mass. Exp Clin Endocrinol Diabetes 2005;113:381–387. [PubMed: 16025399]

99. Moore A, Bonner-Weir S, Weissleder R. Noninvasive In Vivo Measurement of B-Cell Mass in Mouse Model of Diabetes. Diabetes 2001;50:2231–2236. [PubMed: 11574403]

100. Aaen K, Rygaard J, Josefsen K, Petersen H, Brogren C-H, Horn T, Buschard K. Dependence of Antigen Expression on Functional state of B-Cells. Diabetes 1990;39:697–701. [PubMed: 2189761]

101. Brogren C-H, Hirsch F, Wood P, Druet P, Poussier P. Production and characterization of a monoclonal islet cell surface autoantibody from the BB rat. Diabetologia 1986;29:330–333. [PubMed: 3522331]

102. Buschard K, Brogren CH, Ropke C, Rygaard J. Antigen expression of the pancreatic beta-cells is dependent on their functional state, as shown by a specific, BB rat monoclonal autoantibody IC2. Apmis 1988;96:342–346. [PubMed: 3285866]

103. Lal S, Lauer UM, Niethammer D, Beck JF, Schlegel PG. Suicide genes: past, present and future perspectives. Immunol Today 2000;21:48–54. [PubMed: 10637559]

104. Springer CJ, Niculescu-Duvaz I. Prodrug-activating systems in suicide gene therapy. J Clin Invest 2000;105:1161–1167. [PubMed: 10791987]

105. Sun X, Annala AJ, Yaghoubi SS, Barrio JR, Nguyen KN, Toyokuni T, Satyamurthy N, Namavari M, Phelps ME, Herschman HR, Gambhir SS. Quantitative imaging of gene induction in living animals. Gene Ther 2001;8:1572–1579. [PubMed: 11704818]

106. Yaghoubi S, Barrio JR, Dahlbom M, Iyer M, Namavari M, Satyamurthy N, Goldman R, Herschman HR, Phelps ME, Gambhir SS. Human pharmacokinetic and dosimetry studies of [(18)F]FHBG: a reporter probe for imaging herpes simplex virus type-1 thymidine kinase reporter gene expression. J Nucl Med 2001;42:1225–1234. [PubMed: 11483684]

107. Yaghoubi SS, Barrio JR, Namavari M, Satyamurthy N, Phelps ME, Herschman HR, Gambhir SS. Imaging progress of herpes simplex virus type 1 thymidine kinase suicide gene therapy in living subjects with positron emission tomography. Cancer Gene Ther 2005;12:329–339. [PubMed: 15592447]

108. Yaghoubi SS, Wu L, Liang Q, Toyokuni T, Barrio JR, Namavari M, Satyamurthy N, Phelps ME, Herschman HR, Gambhir SS. Direct correlation between positron emission tomographic images of two reporter genes delivered by two distinct adenoviral vectors. Gene Ther 2001;8:1072–1080. [PubMed: 11526454]

109. Lu Y, Dang H, Middleton B, Campbell-Thompson M, Atkinson MA, Gambhir SS, Tian J, Kaufman DL. Long-term monitoring of transplanted islets using positron emission tomography. Mol Ther 2006;14:851–856. [PubMed: 16982215]

110. Proks P, Reimann F, Green N, Gribble F, Ashcroft F. Sulfonylurea stimulation of insulin secretion. Diabetes 2002;51:S368–S376. [PubMed: 12475777]

111. Sweet IR, Cook DL, Lernmark A, Greenbaum CJ, Wallen AR, Marcum ES, Stekhova SA, Krohn KA. Systematic screening of potential beta-cell imaging agents. Biochem Biophys Res Commun 2004;314:976–983. [PubMed: 14751228]

112. Schwanstecher M, Behrends S, Brandt C, Panten U. The binding properties of the solubilized sulfonylurea receptor from a pancreatic B-cell line are modulated by the Mg(++)-complex of ATP. J Pharmacol Exp Ther 1992;262:495–502. [PubMed: 1501109]

113. Schwanstecher M, Brandt C, Behrends S, Schaupp U, Panten U. Effect of MgATP on pinacidil-induced displacement of glibenclamide from the sulphonylurea receptor in a pancreatic beta-cell line and rat cerebral cortex. Br J Pharmacol 1992;106:295–301. [PubMed: 1393263]

114. Schwanstecher M, Loser S, Brandt C, Scheffer K, Rosenberger F, Panten U. Adenine nucleotide-induced inhibition of binding of sulphonylureas to their receptor in pancreatic islets. Br J Pharmacol 1992;105:531–534. [PubMed: 1628141]

115. Schwanstecher M, Schwanstecher C, Dickel C, Chudziak F, Moshiri A, Panten U. Location of the sulphonylurea receptor at the cytoplasmic face of the beta-cell membrane. British Journal of Pharmacology 1994;113:903–911. [PubMed: 7858884]

116. Uhde I, Toman A, Gross I, Schwanstecher C, Schwanstecher M. Identification of the potassium channel opener site on sulfonylurea receptors. J Biol Chem 1999;274:28079–28082. [PubMed: 10497157]

117. Schirrmacher R, Weber MM, Schmitz A, Shiue CY, Alavi AA, Feilen P, Schneider S, Kann P, Rosch F. Radiosynthesis of 1-(4-(2-[^{18}F]fluoroethoxy)benenesulonyl)-3-butyl urea: a potential beta cell imaging agent. J Label Compd Radiopharm 2002;45:763–774.

118. Schmitz A, Shiue CY, Feng Q, Shiue GG, Deng S, Pourdehnad MT, Schirrmacher R, Vatamaniuk M, Doliba N, Matschinsky F, Wolf B, Rosch F, Naji A, Alavi AA. Synthesis and evaluation of fluorine-18 labeled glyburide analogs as beta-cell imaging agents. Nucl Med Biol 2004;31:483–491. [PubMed: 15093819]

119. Schneider S, Feilen PJ, Schreckenberger M, Schwanstecher M, Schwanstecher C, Buchholz HG, Thews O, Oberholzer K, Korobeynikov A, Bauman A, Comagic S, Piel M, Schirrmacher E, Shiue CY, Alavi AA, Bartenstein P, Rosch F, Weber MM, Klein HH, Schirrmacher R. In vitro and in vivo evaluation of novel glibenclamide derivatives as imaging agents for the non-invasive assessment of the pancreatic islet cell mass in animals and humans. Exp Clin Endocrinol Diabetes 2005;113:388–395. [PubMed: 16025400]

120. Kostic BA, Olsen KM, Kearns GL, Kemp SF. Effect of glycated albumin on phenytoin binding in elderly patients with type II diabetes mellitus. Pharmacotherapy 1990;10:362–365. [PubMed: 2235672]

121. Olsen KM, Kearns GL, Kemp SF. Glyburide protein binding and the effect of albumin glycation in children, young adults, and older adults with diabetes. J Clin Pharmacol 1995;35:739–745. [PubMed: 7560255]

122. Wangler B, Beck C, Shiue CY, Schneider S, Schwanstecher C, Schwanstecher M, Feilen PJ, Alavi A, Rosch F, Schirrmacher R. Synthesis and in vitro evaluation of (S)-2-([11C]methoxy)-4-[3-methyl-1-(2-piperidine-1-yl-phenyl)-butyl-carbam oyl]-benzoic acid ([11C]methoxy-repaglinide): a potential beta-cell imaging agent. Bioorg Med Chem Lett 2004;14:5205–5209. [PubMed: 15380228]

123. Wangler B, Schneider S, Thews O, Schirrmacher E, Comagic S, Feilen P, Schwanstecher C, Schwanstecher M, Shiue CY, Alavi A, Hohnemann S, Piel M, Rosch F, Schirrmacher R. Synthesis and evaluation of (S)-2-(2-[18F]fluoroethoxy)-4-([3-methyl-1-(2-piperidin-1-yl-phenyl)-butyl -carbamoyl]-methyl)-benzoic acid ([18F]repaglinide): a promising radioligand for quantification of pancreatic beta-cell mass with positron emission tomography (PET). Nucl Med Biol 2004;31:639–647. [PubMed: 15219283]

124. Bernal-Mizrachi E, Cras-M´eneur C, Ohsugi M, Permutt MA. Gene expression profiling in islet biology and diabetes research. Diabetes Metab Res Rev 2003;19:32–42. [PubMed: 12592642]

125. Abderrahmani A, Niederhauser G, Plaisance Ve, Haefliger J-A, Regazzi R, Waeber G. Neuronal traits are required for glucose-induced insulin secretion. FEBS Letters 2004;565:133–138. [PubMed: 15135066]

126. Komabayashi T, Sawada H, Izawa T, Kogo H. Altered intracellular Ca2+ regulation in pancreatic acinar cells from acute streptozotocin-induced diabetic rats. Eur J Pharmacol 1996;298:299–306. [PubMed: 8846830]

127. Ostenson CG, Grill V. Evidence that hyperglycemia increases muscarinic binding in pancreatic islets of the rat. Endocrinology 1987;121:1705–1710. [PubMed: 3311716]

128. de Lonlay P, Simon-Carre A, Ribeiro MJ, Boddaert N, Giurgea I, Laborde K, Bellanne-Chantelot C, Verkarre V, Polak M, Rahier J, Syrota A, Seidenwurm D, Nihoul-Fekete C, Robert JJ, Brunelle F, Jaubert F. Congenital hyperinsulinism: pancreatic [18F]fluoro-L-dihydroxyphenylalanine (DOPA) positron emission tomography and immunohistochemistry study of DOPA decarboxylase and insulin secretion. J Clin Endocrinol Metab 2006;91:933–940. [PubMed: 16403819]

129. Mohnike K, Blankenstein O, Christesen HT, De Lonlay J, Hussain K, Koopmans KP, Minn H, Mohnike W, Mutair A, Otonkoski T, Rahier J, Ribeiro M, Schoenle E, Fekete CN. Proposal for a standardized protocol for 18F-DOPA-PET (PET/CT) in congenital hyperinsulinism. Horm Res 2006;66:40–42. [PubMed: 16710094]

130. Otonkoski T, Nanto-Salonen K, Seppanen M, Veijola R, Huopio H, Hussain K, Tapanainen P, Eskola O, Parkkola R, Ekstrom K, Guiot Y, Rahier J, Laakso M, Rintala R, Nuutila P, Minn H. Noninvasive diagnosis of focal hyperinsulinism of infancy with [18F]-DOPA positron emission tomography. Diabetes 2006;55:13–18. [PubMed: 16380471]

131. Ribeiro MJ, De Lonlay P, Delzescaux T, Boddaert N, Jaubert F, Bourgeois S, Dolle F, Nihoul-Fekete C, Syrota A, Brunelle F. Characterization of hyperinsulinism in infancy assessed with PET and 18F-fluoro-L-DOPA. J Nucl Med 2005;46:560–566. [PubMed: 15809476]

132. de Lonlay P, Giurgea I, Robert JJ, Fournet JC, Touati G, Nihoul-Fekete C, Brunelle F, Jaubert F, Rahier J, Sempoux C, Junien C, Saudubray JM, Dunne M, Otonkoski T, Ribeiro M, Bellane-Chantelot C. Hyperinsulinemic hypoglycemia in children. Ann Endocrinol (Paris) 2004;65:96–98. [PubMed: 15122102]

133. de Lonlay-Debeney P, Fournet JC, Martin D, Poggi F, Dionisi Vicci C, Spada M, Touati G, Rahier J, Brunelle F, Junien C, Robert JJ, Nihoul-Fekete C, Saudubray JM. [Persistent hyperinsulinemic hypoglycemia in the newborn and infants]. Arch Pediatr 1998;5:1347–1352. [PubMed: 9885743]

134. de Lonlay-Debeney P, Fournet JC, Touati G, Robert JJ, Junien C, Saudubray JM. [Hyperinsulinism]. Arch Pediatr 2001;8:298s–300s. [PubMed: 11394094]

135. de Lonlay-Debeney P, Poggi-Travert F, Fournet JC, Sempoux C, Vici CD, Brunelle F, Touati G, Rahier J, Junien C, Nihoul-Fekete C, Robert JJ, Saudubray JM. Clinical features of 52 neonates with hyperinsulinism. N Engl J Med 1999;340:1169–1175. [PubMed: 10202168]

136. Fekete CN, de Lonlay P, Jaubert F, Rahier J, Brunelle F, Saudubray JM. The surgical management of congenital hyperinsulinemic hypoglycemia in infancy. J Pediatr Surg 2004;39:267–269. [PubMed: 15017535]

137. Filler RM, Weinberg MJ, Cutz E, Wesson DE, Ehrlich RM. Current status of pancreatectomy for persistent idiopathic neonatal hypoglycemia due to islet cell dysplasia. Prog Pediatr Surg 1991;26:60–75. [PubMed: 1904599]

138. Maffei A, Liu Z, Witkowski P, Moschella F, Del Pozzo G, Liu E, Herold K, Winchester RJ, Hardy MA, Harris PE. Identification of tissue-restricted transcripts in human islets. Endocrinology 2004;145:4513–4521. [PubMed: 15231694]

139. Anlauf M, Eissele R, Schafer MK, Eiden LE, Arnold R, Pauser U, Kloppel G, Weihe E. Expression of the two isoforms of the vesicular monoamine transporter (VMAT1 and VMAT2) in the endocrine pancreas and pancreatic endocrine tumors. J Histochem Cytochem 2003;51:1027–1040. [PubMed: 12871984]

140. Weihe E, Eiden LE. Chemical neuroanatomy of the vesicular amine transporters. Faseb J 2000;14:2435–2449. [PubMed: 11099461]

141. Weihe E, Schafer MK, Erickson JD, Eiden LE. Localization of vesicular monoamine transporter isoforms (VMAT1 and VMAT2) to endocrine cells and neurons in rat. J Mol Neurosci 1994;5:149–164. [PubMed: 7654518]

142. DaSilva JN, Carey JE, Sherman PS, Pisani TJ, Kilbourn MR. Characterization of [11C]tetrabenazine as an in vivo radioligand for the vesicular monoamine transporter. Nucl Med Biol 1994;21:151–156. [PubMed: 9234277]

143. Vander Borght TM, Kilbourn MR, Koeppe RA, DaSilva JN, Carey JE, Kuhl DE, Frey KA. In vivo imaging of the brain vesicular monoamine transporter. J Nucl Med 1995;36:2252–2260. [PubMed: 8523116]

144. Mori T. Cancer-specific ligands identified from screening of peptide-display libraries. Curr Pharm Des 2004;10:2335–2343. [PubMed: 15279612]

145. Stefanidakis M, Koivunen E. Peptide-mediated delivery of therapeutic and imaging agents into mammalian cells. Curr Pharm Des 2004;10:3033–3044. [PubMed: 15379666]

146. Samli KN, McGuire MJ, Newgard CB, Johnston SA, Brown KC. Peptide-mediated targeting of the islets of Langerhans. Diabetes 2005;54:2103–2108. [PubMed: 15983211]

147. Hohmeier HE, Mulder H, Chen G, Henkel-Rieger R, Prentki M, Newgard CB. Isolation of INS-1-derived cell lines with robust ATP-sensitive K+ channel-dependent and -independent glucose-stimulated insulin secretion. Diabetes 2000;49:424–430. [PubMed: 10868964]

148. Tsyganov EN, Anderson J, Arbique G, Constantinescu A, Jennewein M, Kulkarni P, Mason RP, McColl RW, Oz OK, Parkey RW, Richer E, Roesch F, Seliounine SY, Slavine NV, Srivastava SC, Thorpe PE, Zinchenko AI, Antich PP. UTSW small animal positron emission imager. EEE Trans. Nucl. Sci 2006;53:2591–2600.

149. Slavine NV, Lewis MA, Richer E, Antich PP. Iterative reconstruction method for light emitting sources based on the diffusion equation. Med Phys 2006;33:61–68. [PubMed: 16485410]

150. Li S, Liu Y-H, Oyama T, McGuire MJ, Brown KC. Facile synthesis of multimeric peptides: Developmeny of cell-specific delivery systems. Angew Chem Int Ed. 2007in press

151. Oyama T, Sykes KF, Samli KN, Minna JD, Johnston SA, Brown KC. Isolation of lung tumor specific peptides from a random peptide library: generation of diagnostic and cell-targeting reagents. Cancer Lett 2003;202:219–230. [PubMed: 14643452]

152. Zhou X, Chang YC, Oyama T, McGuire MJ, Brown KC. Cell-specific delivery of a chemotherapeutic to lung cancer cells. J Am Chem Soc 2004;126:15656–15657. [PubMed: 15571383]

153. De J, Chang YC, Samli KN, Schisler JC, Newgard CB, Johnston SA, Brown KC. Isolation of a mycoplasma-specific binding peptide from an unbiased phage-displayed peptide library. Mol Biosyst 2005;1:149–157. [PubMed: 16880978]

154. McGuire MJ, Samli KN, Chang YC, Brown KC. Novel ligands for cancer diagnosis: selection of peptide ligands for identification and isolation of B-cell lymphomas. Exp Hematol 2006;34:443–452. [PubMed: 16569591]

155. McGuire MJ, Sykes KF, Samli KN, Timares L, Barry MA, Stemke-Hale K, Tagliaferri F, Logan M, Jansa K, Takashima A, Brown KC, Johnston SA. A library-selected, Langerhans cell-targeting peptide enhances an immune response. DNA Cell Biol 2004;23:742–752. [PubMed: 15585132]

156. Oyama T, Rombel IT, Samli KN, Zhou X, Brown KC. Isolation of multiple cell-binding ligands from different phage displayed-peptide libraries. Biosens Bioelectron 2006;21:1867–1875. [PubMed: 16386888]

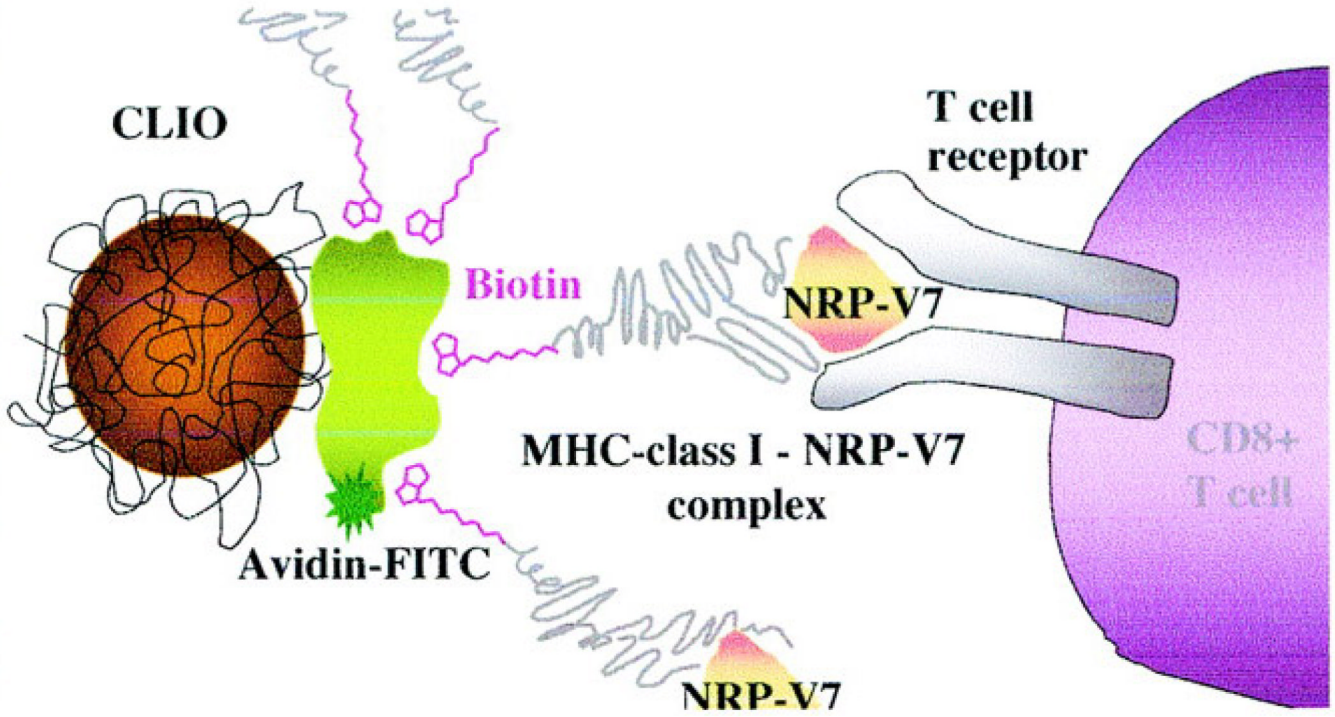

Figure 1.
Schematic CLIO-NRP-V7 probe. Biotinylated NRP-V7/H-2Kd complex was coupled to CLIO particles modified with avidin. CLIO-NRP-V7 probe is recognized by the TCR on NRP-V7-reactive $CD8^+$ T-cells. (Copyright © 2007 American Diabetes Association. From Diabetes®, Vol. 53, 2004; 1459–1466. Reprinted with permission from the American Diabetes Association.)

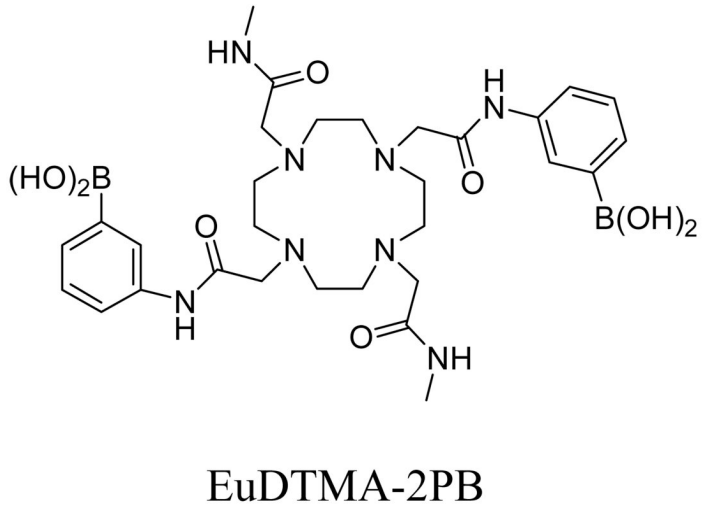

EuDTMA-2PB

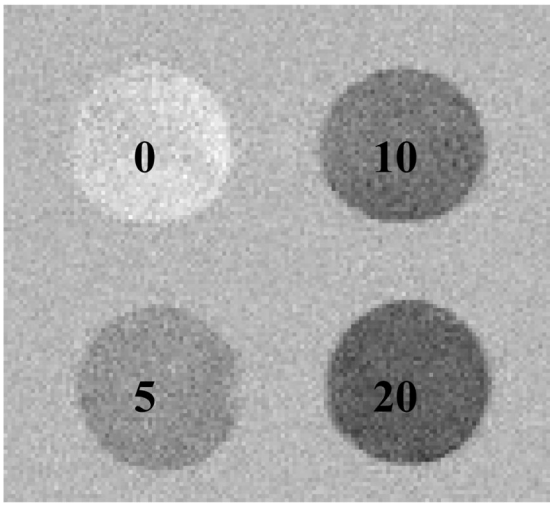

Figure 2.
CEST images of 10 mM EuDTMA-2PB in the presence of 0, 5, 10 or 20 mM glucose. The images were obtained by subtraction after a 2s presaturation pulse at either 30 or 50 ppm.

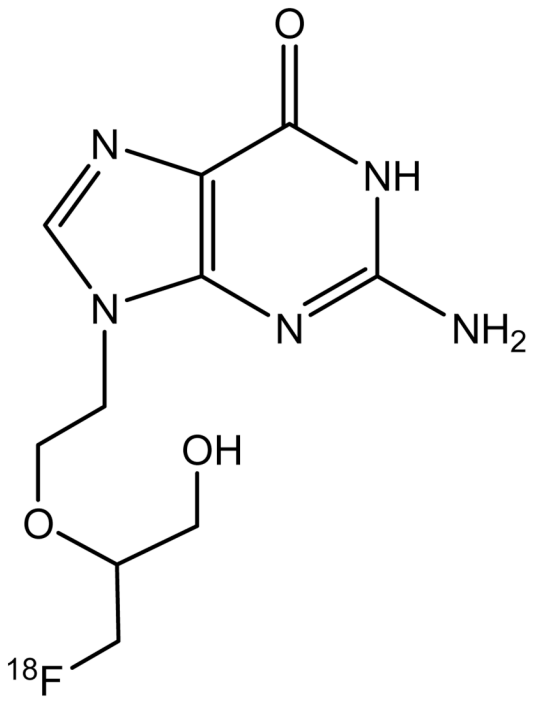

18F-FHBG

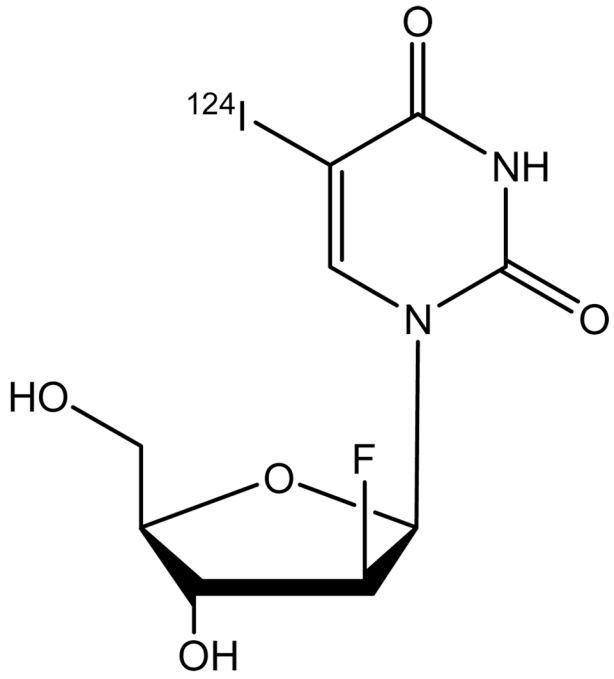

124I-FIAU

Figure 3.
Chemical structures of ^{18}F-FHBG and ^{124}I-FIAU.

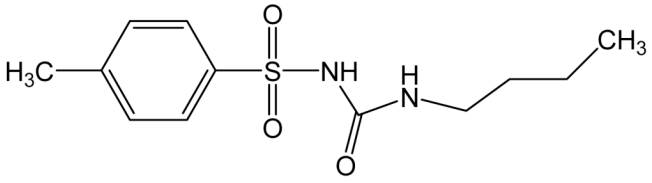

Tolbutamide

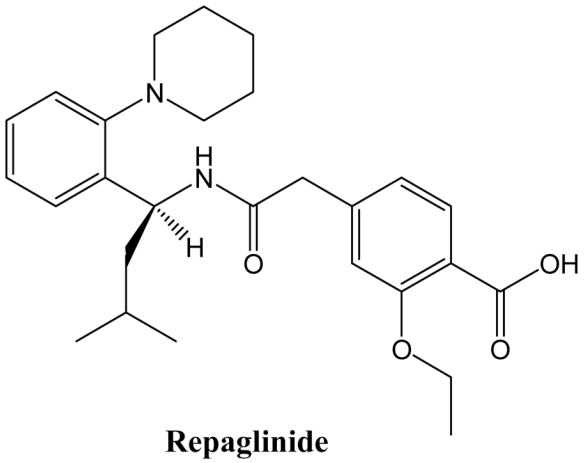

Repaglinide

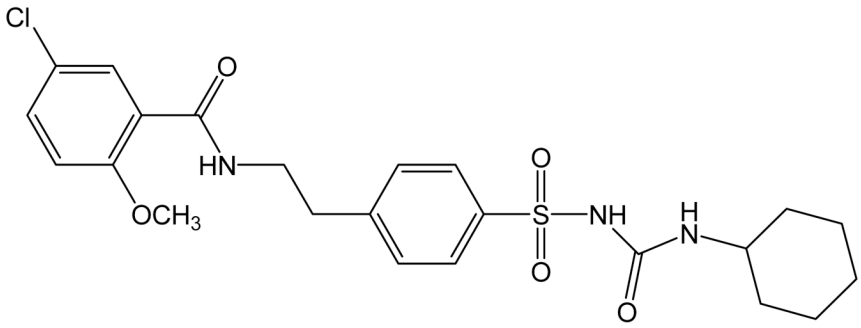

Glibenclamide

Figure 4.
Chemical structures of glibenclamide, tolbutamide, and repaglinide.

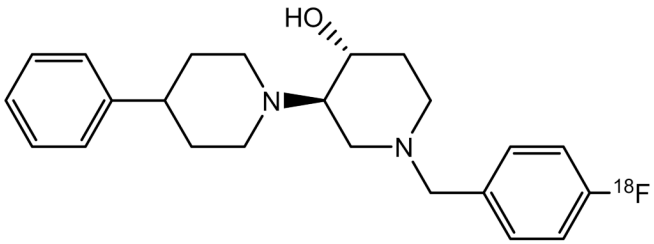

4-^{18}F-Fluoro-Benzyltrozamicol (FBT)

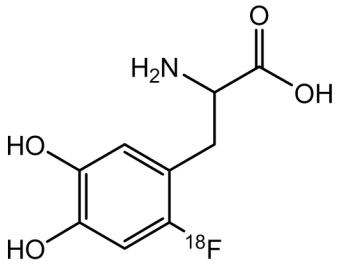

^{18}F-Fluoro-L-DOPA

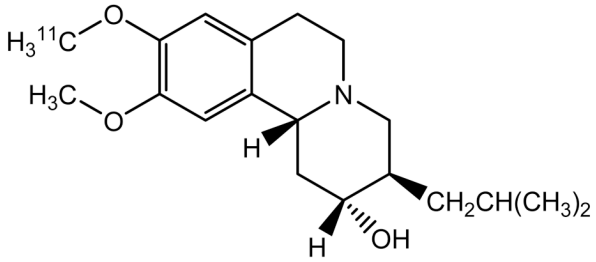

^{11}C-Dihydrotetrabenazine (DTBZ)

Figure 5.
Chemical structures of ^{18}F-FBT, ^{11}C-DTBZ, and ^{18}F-fluoro-L-DOPA.

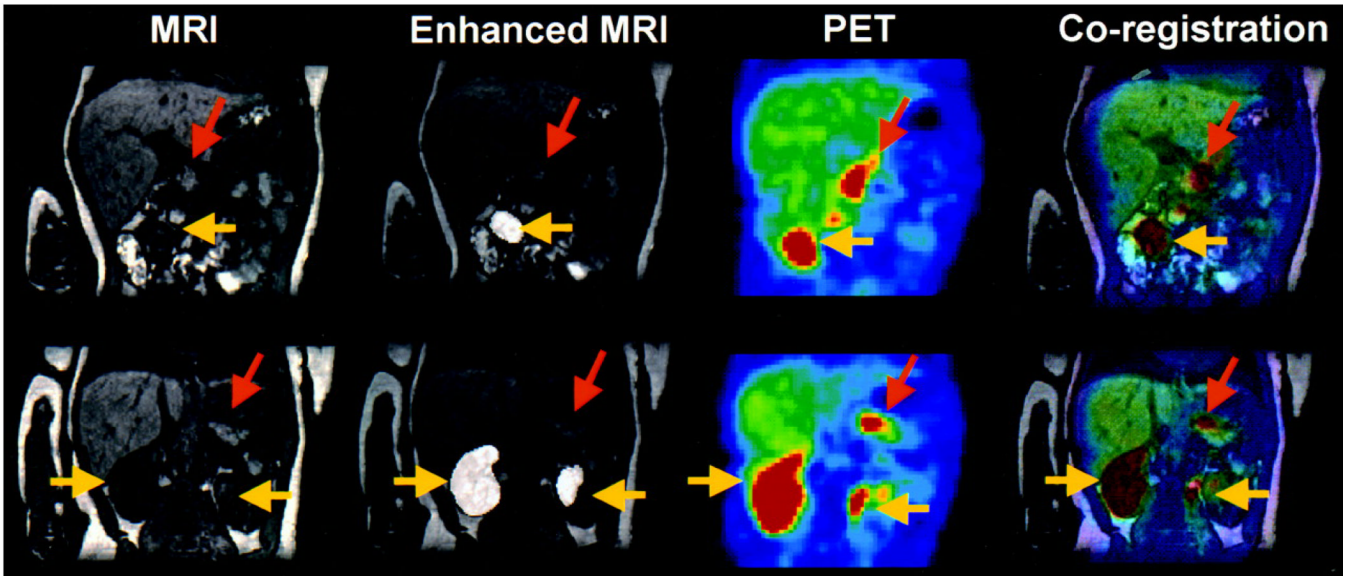

Figure 6.
MRI, enhanced MRI, PET, and resultant coregistration images obtained from a patient with diffuse hyperinsulinism. Coregistration images confirm diffuse uptake of ^{18}F-labeled-L-DOPA by the pancreas (orange arrows: pancreas; yellow arrows: kidneys). (Reprinted by permission of the Society of Nuclear Medicine from: Maria-João Ribeiro, Pascale De Lonlay, Thierry Delzescaux, Nathalie Boddaert, Francis Jaubert, Sandrine Bourgeois, Frédéric Dollé, Claire Nihoul-Fékété, André Syrota, and Francis Brunelle. Characterization of Hyperinsulinism in Infancy Assessed with PET and ^{18}F-Fluoro-L-DOPA. J Nucl Med. 2005 46(4): 560–566).

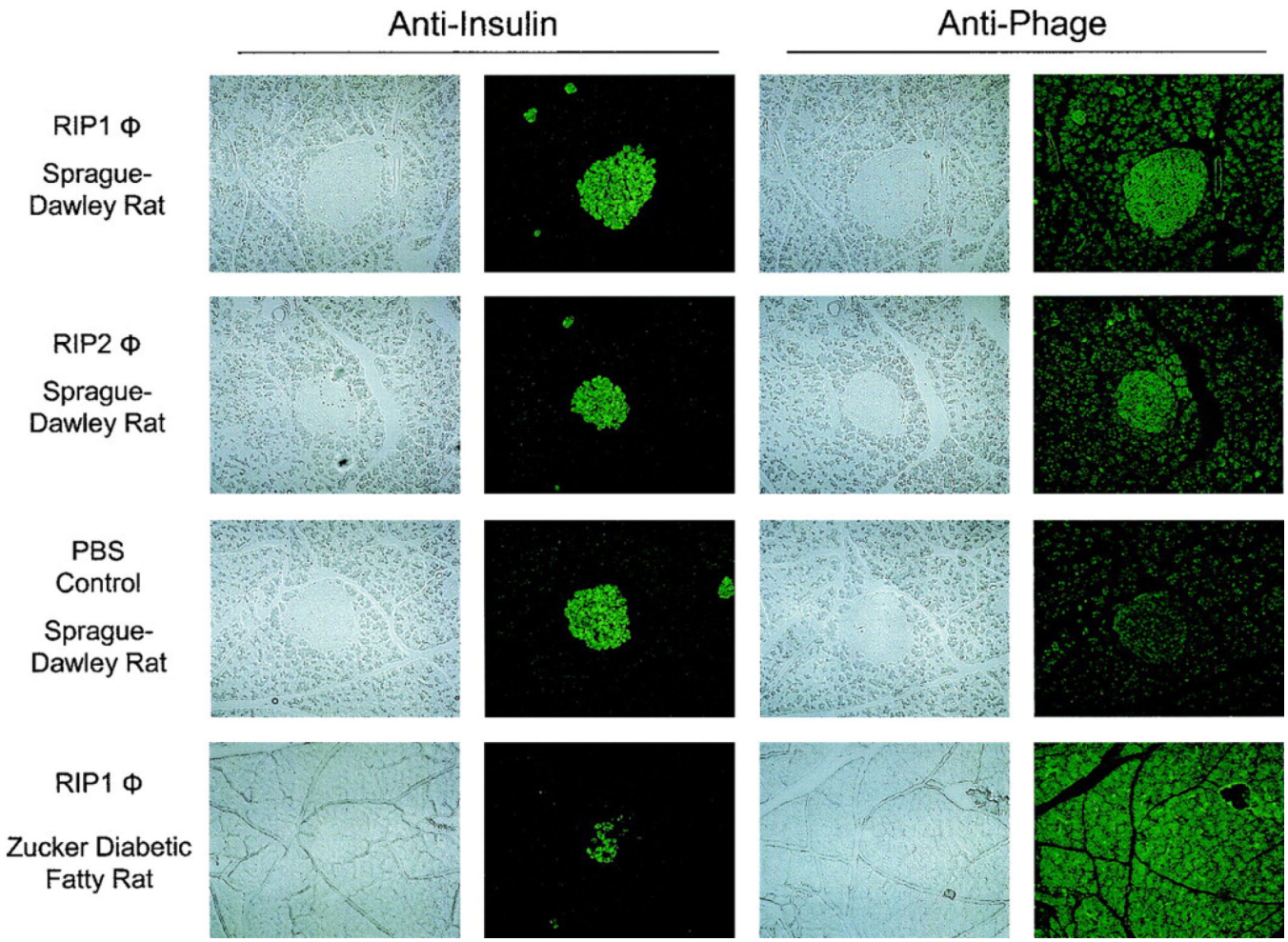

Figure 7.

Distribution of RIP1 and RIP2 phage in the pancreata from Sprague-Dawley or ZDF rats. The phage was injected intravenously into the jugular vein and allowed to circulate for 2 h. Aligned sections are shown staining with anti-insulin or anti-phage antibodies. All panels are at 100 × magnification. Significant accumulation of RIP1 and RIP2 phage in the islets of the Sprague-Dawley rats is visible. No significant accumulation of RIP1 phage is seen within the islet of a ZDF rat. (Copyright © 2005 American Diabetes Association. From Diabetes®, Vol. 54, 2005; 2103–2108. Reprinted with permission from the American Diabetes Association.)

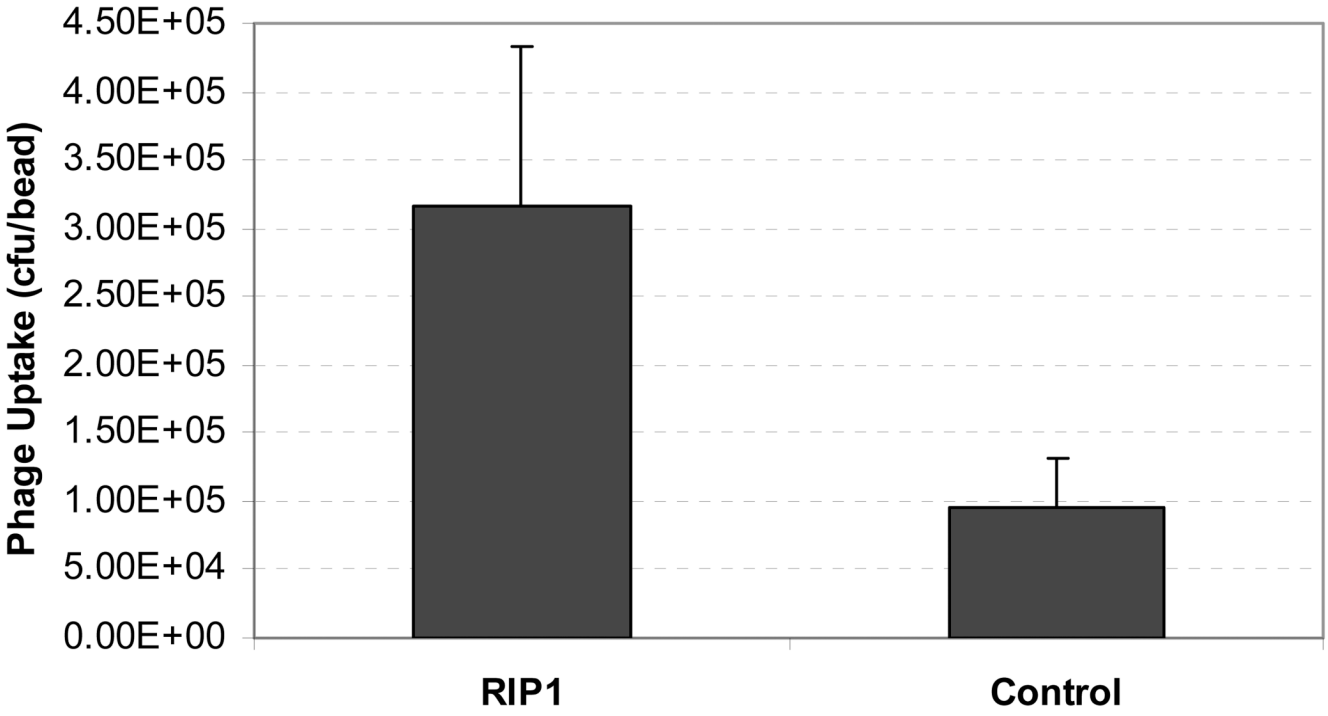

Figure 8.
Uptake of ^{125}I labeled RIP1 and control phage clone in islet-embedded alginate beads (n = 5). Data are presented as mean ± s.d.

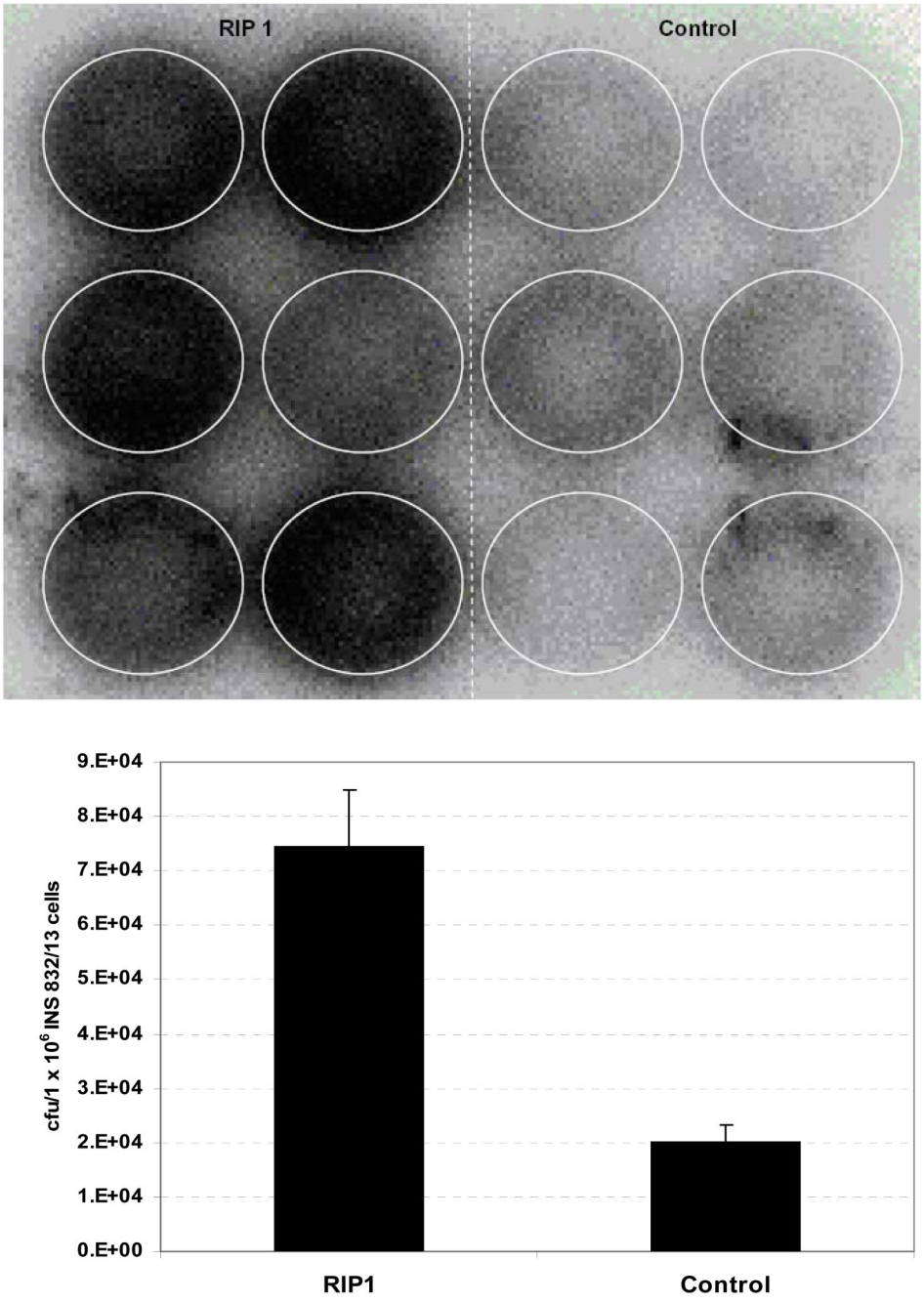

Figure 9.

INS 832/13 cell uptake of ^{125}I labeled RIP1 and control phage clones. Upper panel: autoradiographic image of a 12-well plate. Left six wells: ^{125}I labeled RIP1 phage; right six wells: ^{125}I labeled control phage. Lower panel: Gamma counts of the INS 832/13 cells associated RIP1 and control phage clones (n = 6). Data are presented as mean ± s.d.

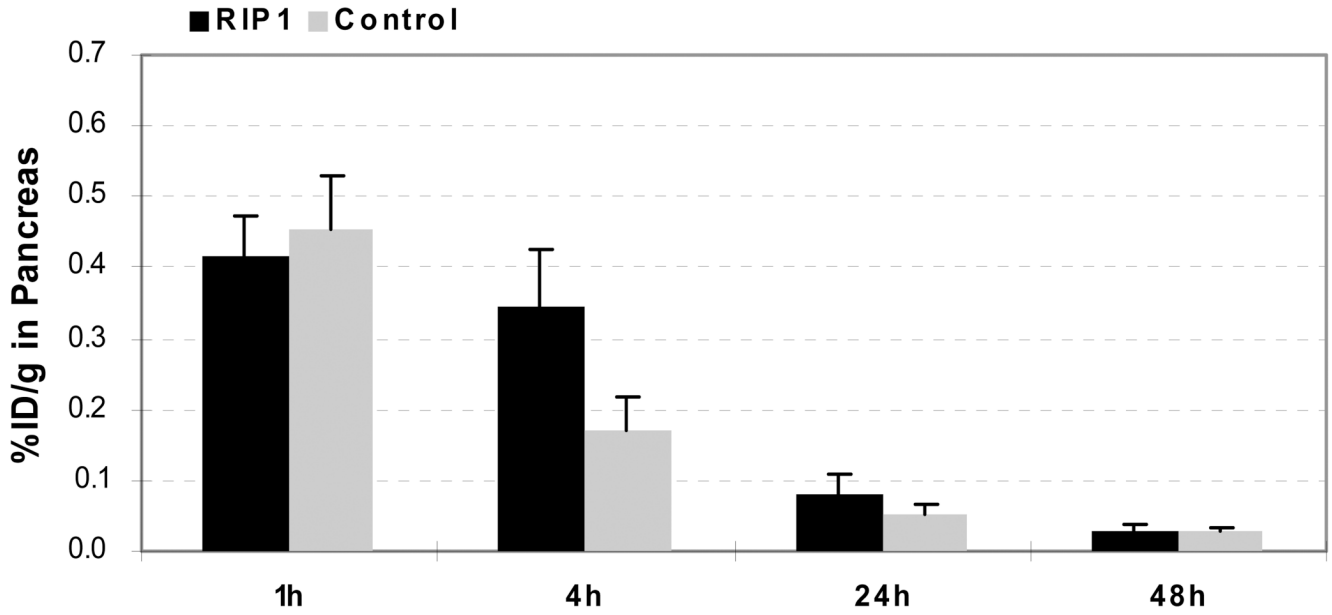

Figure 10.
Comparative biodistribution data of ^{125}I labeled RIP1 and control phage clones in pancreas uptake at 1, 4, 24, and 48 h p.i (n = 4). Data are presented as mean ± s.d.

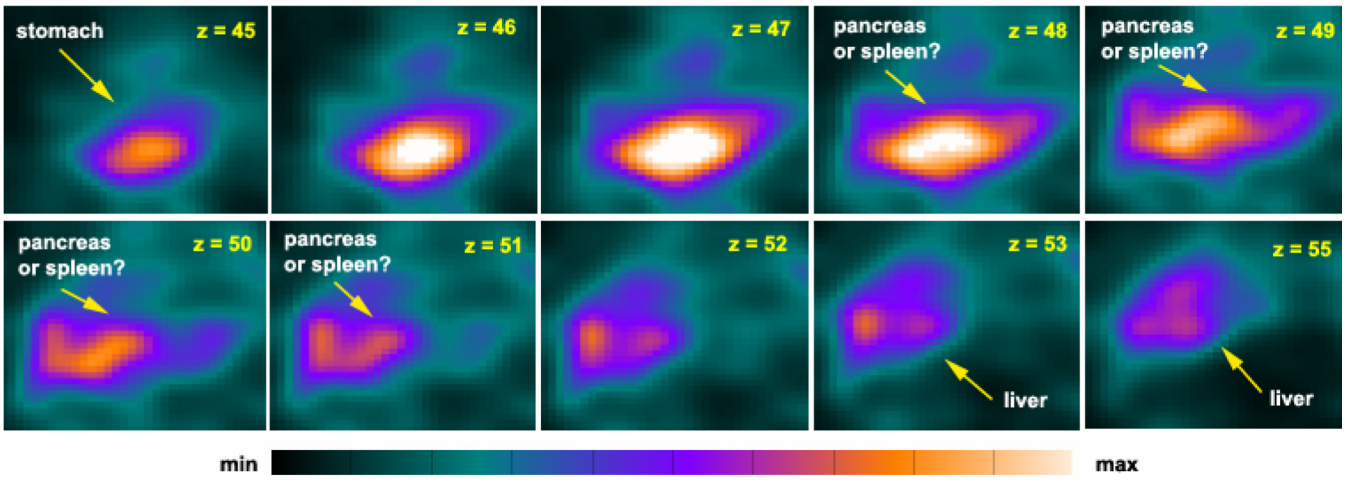

Figure 11.
PET imaging with ^{124}I-labeled RIP1 phage in a healthy Sprague-Dawley rat (183 g) at 4 h p.i. Coronal image slices (1-mm thick) from posterior (z = 45) to anterior (z = 56).

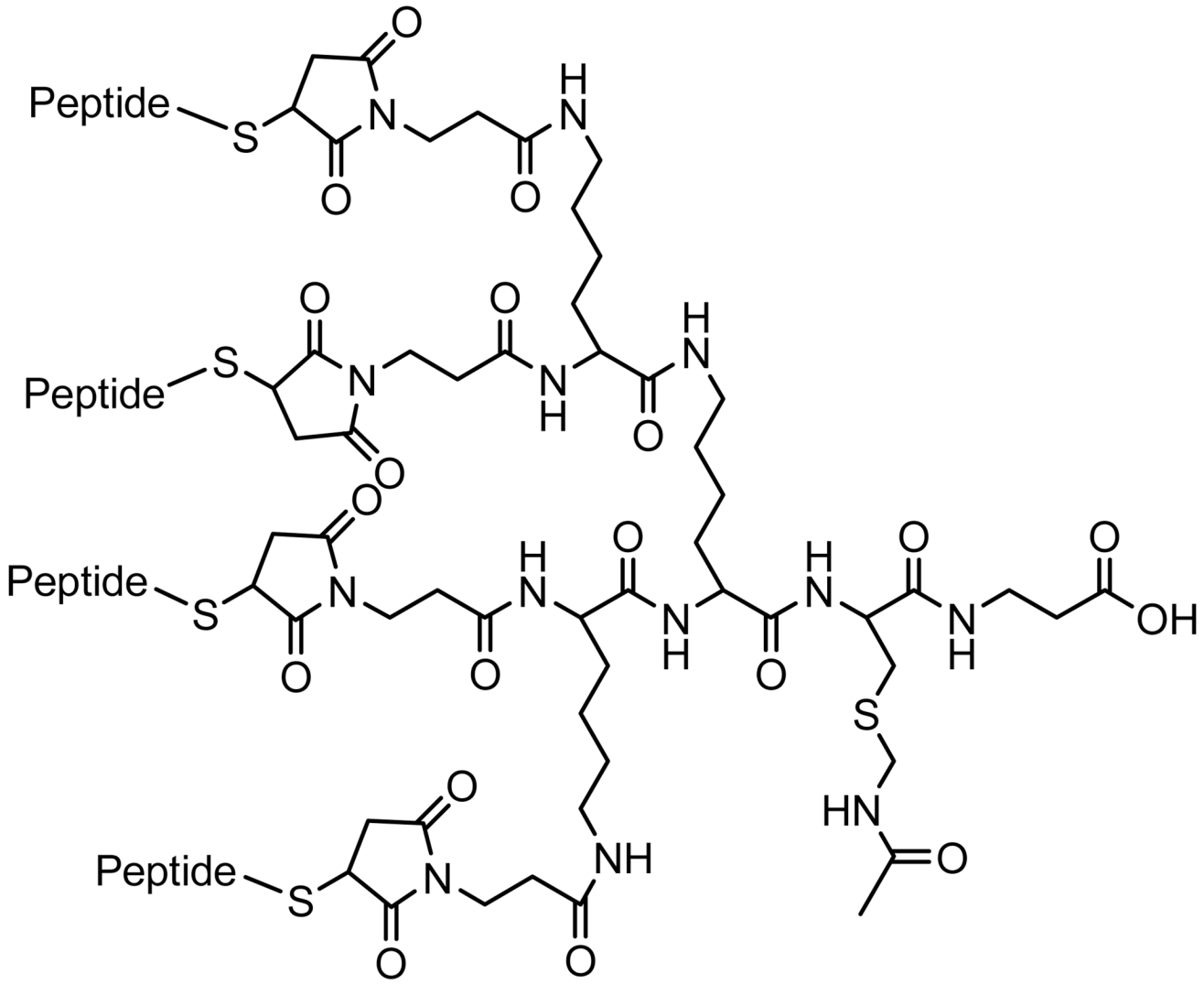

RIP1 peptide sequence: LSGTPERSGQAVKVKLKAIP

Figure 12.
A typical construct for a tetrameric peptide.